JOURNAL OF GEOPHYSICAL RESEARCH, VOL. 102, NO. D11, PAGES 13,235–13,253, JUNE 20, 1997

Evolution and stoichiometry of heterogeneous processing in the Antarctic stratosphere

L. Jaeglé,[1,2] C. R. Webster,[3] R. D. May,[3] D. C. Scott,[3] R. M. Stimpfle,[4] D.W. Kohn,[4] P. O. Wennberg,[4] T. F. Hanisco,[4] R. C. Cohen,[4] M. H. Proffitt,[5] K. K. Kelly,[5] J. Elkins,[6] D. Baumgardner,[7] J. E. Dye,[7] J. C. Wilson,[8] R. F. Pueschel,[9] K. R. Chan,[9] R. J. Salawitch,[3] A. F. Tuck,[5] S. J. Hovde,[5] Y. L. Yung[10]

Abstract. Simultaneous in situ measurements of HCl and ClO have been made for the first time in the southern hemisphere, allowing a systematic study of the processes governing chlorine activation between 15 and 20 km in the 1994 Antarctic winter. Data for several other gases (O_3, NO, NO_y, OH, HO_2, N_2O, CH_4, CO, H_2O, CFCs), particulates, and meteorological parameters were collected from the ER-2 aircraft out of New Zealand as part of the 1994 Airborne Southern Hemisphere Ozone Experiment/Measurements of Atmospheric Effects of Stratospheric Aircraft (ASHOE/MAESA) campaign. Observations from the ER-2 in the fall (April-May), prior to polar night, show that chlorine activation begins with 60-75% of inorganic chlorine as HCl. By midwinter (July-August), near-total removal of HCl is observed. The wintertime loss of HCl in air recently exposed to extreme temperatures is found to be correlated with high levels of reactive chlorine (ClO and its dimer, Cl_2O_2) in the linear fashion expected from the stoichiometry of the heterogeneous reaction of hydrochloric acid with chlorine nitrate on polar stratospheric clouds (PSCs): $HCl + ClONO_2 \rightarrow Cl_2 + HNO_3$. To constrain the role of different heterogeneous reactions and PSC types, we have used a photochemical trajectory model which includes heterogeneous sulfate and PSC chemistry. Model calculations of the evolution of reactive gases are compared with the in situ observations. In addition, simultaneous measurements of OH and HO_2 are used as a diagnostic for the occurrence of the heterogeneous reaction $HOCl + HCl \rightarrow Cl_2 + H_2O$, which contributes to suppressed levels of HO_x inside the vortex. It is shown that the amount of chlorine activation is not strongly dependent on the composition of PSCs. However, HO_x levels exhibit different signatures depending on the type of heterogeneous surfaces that affected chlorine activation. Furthermore, this analysis implies that in the edge region of the Antarctic vortex, the observed near-total removal of HCl can result from latitudinal excursions of air parcels in and out of sunlight during the winter, which photochemically resupply HOCl and $ClONO_2$ as oxidation partners for HCl.

1. Introduction

Stratospheric inorganic chlorine (Cl_y = HCl + $ClONO_2$ + HOCl + ClO + 2 Cl_2O_2 + OClO + 2 Cl_2 + Cl) is produced primarily from the emission of man-made chlorofluorocarbons (CFCs) and hydrofluorocarbons (HCFCs) at the surface of the Earth followed by transport to the stratosphere where their photochemical breakdown releases chlorine atoms [*Molina and Rowland*, 1974]. At middle and low latitudes, inorganic chlorine is mainly composed of the stable inactive reservoir forms HCl and $ClONO_2$. During the Antarctic winter, abrupt and sustained shifts in the partitioning of chlorine from HCl and $ClONO_2$ to photochemically reactive chlorine forms (or Cl_x = ClO + Cl + 2 Cl_2O_2 + 2 Cl_2 + OClO) occur as a result of heterogeneous conversion on the surfaces of polar stratospheric cloud particles [*Solomon et al.*, 1986; *Crutzen and Arnold*, 1986]. The high levels of reactive chlorine throughout the polar winter initiate massive ozone loss in the Antarctic polar spring [*Farman et al.*, 1985; *Hofmann et al.*, 1994]. Many observational studies [*Tuck et al.*, 1989; *Anderson et al.*, 1991; *Toohey et al.*, 1993; *Webster et al.*, 1993; *Waters et al.*, 1993; *Pyle et al.*, 1994] as well as gas phase and heterogeneous laboratory studies [*Molina and Molina*, 1987; *Tolbert et al.*, 1987; *Leu*, 1988] have helped elucidate the mechanisms for heterogeneous processing and for the gas phase catalytic cycles ultimately responsible for the springtime ozone loss. The integration of this accumulated set of data has allowed modeling studies of these processes [*Crutzen et al.*, 1992; *Salawitch et al.*, 1993; *Lefèvre et al.*, 1994; *Chipperfield et al.*, 1995].

[1]Environmental Engineering Science Division, California Institute of Technology, Pasadena
[2]Now at Harvard University, Department of Earth and Planetary Sciences, Cambridge, Massachusetts
[3]Atmospheric Chemistry Division, Jet Propulsion Laboratory, California Institute of Technology, Pasadena
[4]Department of Chemistry, Harvard University, Cambridge, Massachusetts.
[5]Aeronomy Laboratory, NOAA, Boulder, Colorado.
[6]Climate Monitoring and Diagnostic Laboratory, NOAA, Boulder, Colorado.
[7]National Center for Atmospheric Research, Boulder, Colorado.
[8]Department of Engineering, University of Denver, Denver, Colorado.
[9]NASA Ames Research Center, Moffett Field, California.
[10]Division of Geological and Planetary Sciences, California Institute of Technology, Pasadena

Paper number 97JD00935.
0148-0227/97/97JD-00935.$09 00

In our current understanding of the polar stratosphere, three principal heterogeneous reactions are believed to convert inorganic chlorine reservoirs to Cl_x [*Solomon*, 1990]:

$$HCl + ClONO_2 \rightarrow Cl_2 + HNO_3 \quad (1)$$
$$ClONO_2 + H_2O \rightarrow HOCl + HNO_3 \quad (2)$$
$$HCl + HOCl \rightarrow Cl_2 + H_2O. \quad (3)$$

The surfaces on which these reactions take place are provided by the particles making up polar stratospheric clouds (PSCs) [*McCormick et al.*, 1982], which are believed to be $HNO_3/H_2SO_4/H_2O$ systems of different compositions and phases [*Carslaw et al.*, 1994; *Tabazadeh et al.*, 1994], and form at the cold temperatures typical of the winter polar vortex. The gaseous products of reactions (1)-(3), Cl_2, and HOCl (which are seen to desorb from the PSC surfaces in laboratory observations) are rapidly converted to ClO and Cl_2O_2, the two dominant forms of Cl_x in the polar winter stratosphere [*Anderson et al.*, 1991]. The occurrence of reaction (1) is supported by the stoichiometry of HCl loss and ClO production from in situ observations in the Arctic [*Webster et al.*, 1993]. After the eruption of Mount Pinatubo, high levels of OClO were observed in the Antarctic vortex and were attributed to chlorine activation via reaction (2) on volcanic sulfate aerosols [*Solomon et al.*, 1993].

In addition to providing sites for heterogeneous chemical reactions, PSCs can sequester a significant fraction of stratospheric HNO_3 in condensed forms [*Toon et al.*, 1986]. Growth and subsequent sedimentation of these particles lead to denitrification, further enhancing ozone loss [*Fahey et al.*, 1990]. Indeed, while chlorine radicals control the rate at which ozone is being destroyed, the duration of the destruction of O_3 is limited by the resupply of reactive nitrogen which sequesters Cl_x in the form of $ClONO_2$ [*Salawitch et al.*, 1988]. Given photochemical decomposition of HNO_3 to NO_2 under sufficient levels of sunlight, conversion of ClO back to $ClONO_2$ can take place via

$$ClO + NO_2 + M \rightarrow ClONO_2 + M. \quad (4)$$

HCl itself is reformed through the reaction

$$Cl + CH_4 \rightarrow HCl + CH_3. \quad (5)$$

Thus understanding the factors controlling chlorine activation and deactivation is central to predicting ozone loss rates in the polar regions.

In this paper, we present simultaneous in situ measurements of HCl and ClO in the Antarctic lower stratosphere during the fall and winter 1994, which were carried out as part of the Airborne Southern Hemisphere Ozone Experiment /Measurements of Atmospheric Effects of Stratospheric Aircraft (ASHOE/MAESA) campaign [*Tuck et al.*, 1997]. Observations of HCl and ClO, in combination with the other reactive gases measured (OH, HO_2, NO) and complemented by aerosol measurements as well as observations of precursors and tracers, constitute a powerful set of indicators on the impact of chlorine chemistry in the perturbed environment of the polar vortex. The first simultaneous in situ measurements of HCl and ClO in the Antarctic provide additional insight into the heterogeneous processes taking place in a vortex generally colder and more extensive than that of the Arctic. While ClO by itself reflects largely the amount of recent processing that has taken place, HCl, on the other hand, keeps a much longer "memory" of the heterogeneous conversion because of its very slow recovery, and provides a useful measure of the accumulated effect of chlorine activation. Furthermore the simultaneous in situ measurements of HO_x species during ASHOE/MAESA allow a unique assessment of the occurrence of reactions (2) and (3) in the stratosphere (D.W. Kohn et al., manuscript submitted to J. Geophys. Res.: "Constraints on sulfate aerosol reactions along back trajectories imposed by HO_x and ClO_x in situ measurements", 1996) (hereinafter referred to as K96).

To interpret the chemical and dynamical factors affecting the chemical composition of the stratosphere during the Antarctic winter, this study uses a photochemical box model along trajectories. Because this approach takes into account the temperature history of an air parcel, it has already proved useful in studying stratospheric chemistry under polar conditions [*Austin et al.*, 1989; *Jones et al.*, 1989; *Schoeberl et al.*, 1993; *Lutman et al.*, 1994a, b]. In particular, trajectory models compared well with satellite and in situ observations of high ClO levels [*Jones et al.*, 1989; *Lutman et al.*, 1994a] and quantitatively predicted the relaxation of these enhanced ClO concentrations following encounters with PSCs [*Schoeberl et al.*, 1993; *Lutman et al.*, 1994b].

We begin in section 2 by briefly describing the data collected by instruments aboard the ER-2 during ASHOE/MAESA. Sections 3 and 4 will present observations of the conversion of chlorine reservoirs to reactive chlorine and how these can be analyzed to gain quantitative information on the stoichiometry of the processes responsible for chlorine activation. We describe the Lagrangian photochemical model in section 5. In sections 6 and 7, model simulation results are presented and compared with observations. We conclude by presenting in section 8 a summary of the results obtained in this investigation.

2. Observations and Instruments

The Aircraft Laser Infrared Absorption Spectrometer (ALIAS) instrument is a scanning tunable diode laser spectrometer [*Webster et al.*, 1994] which measures HCl [*Webster et al.*, 1993], CO, N_2O, and CH_4, using high-resolution laser absorption at wavelengths from 3 to 8 μm in an 80-m multipass cell. The measurement uncertainty depends on signal size as well as on uncertainties in spectral parameters. The total uncertainty (1σ) for 30 s averages of HCl is typically 10% at 1 ppbv and 30% for the mixing ratios below 0.3 ppbv. The minimum detectable HCl amount is about 0.1 ppbv, although in some flights, this can be as low as 0.05 ppbv. Table 1 briefly summarizes information on the other instruments onboard the ER-2. In addition, temperature and pressure are measured by the meteorological measurement system instrument [*Scott et al.*, 1990] with accuracies of ±0.3 mbar and ±0.3 K.

The series of flights discussed here were part of the ASHOE/MAESA mission, between the months of April and October of 1994. In southern flights out of Christchurch, New Zealand (44°S, 172°E), the ER-2 aircraft typically sampled air from 15 km (~120 mbar) to 20 km (~55 mbar). The length of the flights is limited to 8 hours, and therefore from Christchurch, the ER-2 predominantly sampled the edge region of the Antarctic vortex. Southern flights generally penetrated ~1°-3° of latitude inside the vortex up to ~ 70°S.

3. Chlorine Activation and Recovery

In this section, we first describe observations of the chlorine partitioning prior to polar night (April-May), deriving empirical relations for reference levels that will allow us to assess the amount of change in HCl and $ClONO_2$ when heterogeneous processing takes place during the winter. We then present HCl

Table 1. Instruments Onboard the ER-2

Observed Quantities	Techniques	Accuracy (1σ, %)	Reference
HCl, N_2O, CH_4, CO	tunable diode-laser absorption	10, 5, 5, 10	*Webster et al.* [1994]
ClO	resonance fluorescence	15	*Brune et al.* [1989]
NO, NO_y	NO/O_3 chemiluminescence	15, 15	*Fahey et al.* [1989]
OH, HO_2	laser-induced fluorescence	30, 40	*Wennberg et al.* [1994]
CFCs	gas chromatograph	3	*Elkins et al.* [1996]
O_3	differential UV absorption	5	*Proffitt et al.* [1989]
H_2O	lyman-α hygrometer	10	*Kelly et al.* [1989]
Aerosols (0.06-0.2 μm)	focused cavity spectrometer	100	*Jonsson et al.* [1995]
Aerosols (0.2 - 20 μm)	multi angle spectrometer	100	*Baumgardner et al.* [1992]
Aerosol composition	impactor	100	*Pueschel et al.* [1989]

and ClO measurements during the flight of August 6, 1994, during which processed air was encountered. Finally, we summarize the evolution the HCl and ClO observations spanning the four ASHOE/MAESA phases from April to October 1994.

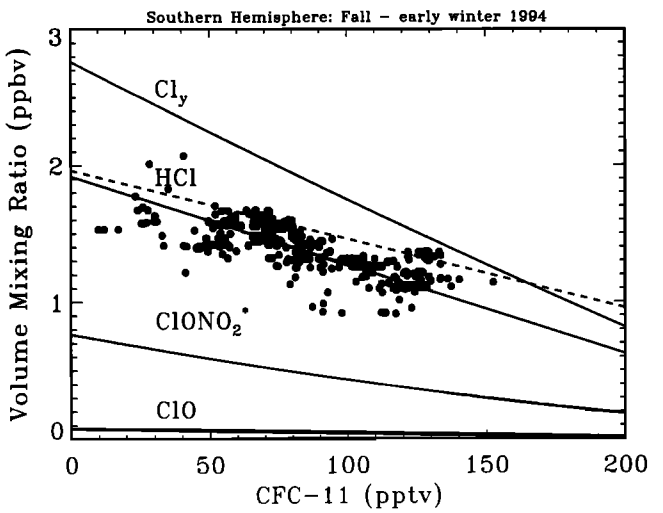

Figure 1. Unperturbed Antarctic atmosphere: partitioning of chlorine species observed in the fall and early winter 1994, represented as a function of CFC-11. Four flights were used for the HCl data (circles): April 13, May 23, and 24, and June 1, 1994 (latitude between 40°S and 68°S). The relationship obtained (solid line) is $HCl^*(CFC\text{-}11) = 1.92 - 6.5 \times 10^{-3}$ CFC-11 $+1.85 \times 10^{-8}$ $(CFC\text{-}11)^2$, with HCl in ppbv, and CFC-11 in pptv When no CFC-11 measurements are available, an empirical relation between N_2O and CFC-11 is used instead CFC-11 (pptv) $= 3.514 \times 10^{-1} (N_2O)^2 - 8.82 \times 10^{-3} N_2O - 54.47$, N_2O in ppbv). Cl_y is based on interpolated measurements of organic halogens (Cl_y (ppbv) $= 4.05 \times 10^{-6}$ $(CFC\text{-}11)^2 - 1.056 \times 10^{-2}$ CFC-11 + 2.76, CFC-11 in pptv). A fit to ClO observations is also shown as well as the inferred chlorine nitrate: $ClONO_2^* = Cl_y - HCl - ClO - HOCl^*$. The relationship obtained is $ClONO_2^*(CFC\text{-}11) = 0.764 - 0.0037 \times$ CFC-11 $+ 4.0 \times 10^{-6}$ $(CFC\text{-}11)^2$. The data were selected for pressures < 80 mbar, and ClO < 50 pptv. The dashed line corresponds to the HCl(CFC-11) relationship for the northbound flight of May 28, 1994.

3.1. Initial Partitioning

At midlatitudes away from polar processing, most of inorganic chlorine is in the form of its reservoirs, HCl and $ClONO_2$, with small contributions from ClO and HOCl. In order to identify chemical changes in either the chlorine reservoirs (HCl and $ClONO_2$) or the radical (ClO) in an air parcel, we need to establish the expected amounts of these species relative to a dynamical tracer such as N_2O or CFC-11. Figure 1 shows the HCl mixing ratios as a function of CFC-11 for four ER-2 flights between April and early June. The observed correlation of HCl with CFC-11 is due to the direct relationship between the source gas and the main inorganic chlorine reservoir, as well as to the fact that HCl mixing ratios are mostly controlled at these altitudes by O_3 and CH_4 which themselves have tight correlations with CFC-11 [*Plumb and Ko*, 1992; *Chan et al.*, 1996].

We will assume ER-2 observations in the fall to be representative of the unperturbed atmosphere. A potential problem with this approach is that the air sampled by the ER-2 later during the winter (in July-August) most likely originated from higher altitudes as a result of descent within the vortex [*Schoeberl et al.*, 1995]. Current estimates of descent rates inside the Antarctic vortex range between 0.02 and 0.07 cm s^{-1} [World Meteorological Organization (WMO), 1995], suggesting that air could have descended by 2 km to a maximum of 7 km between April and August. To assess the impact of descent on HCl/tracer relationships, we have examined HCl and CH_4 profiles obtained by the Halogen Occultation Experiment (HALOE) [*Russell et al.*, 1993] aboard the Upper Atmospheric Research Satellite (UARS) in March 1994 (70°-74°S). The correlation between HCl and CH_4 obtained with these HALOE observations between 20 and 28 km is about 10% lower than the ER-2 correlation, well within the respective uncertainties of these instruments (J. Russell, personal communication, 1996). These satellite observations thus show that descent whithin the Antarctic vortex does not greatly affect the initial chlorine partitioning illustrated by the correlations in Figure 1.

The total inorganic chlorine, Cl_y, expected in an air parcel is based on organic chlorine measurements aboard the ER-2 and is calculated for each CFC-11 value (or N_2O, when no CFC-11 observations are available) using SF_6 to calculate the mean age of

the air mass [*Elkins et al.*, 1996]. The estimated uncertainty on the derived Cl_y is 20% [*Woodbridge et al.*, 1992]. Flights north of Christchurch (45°-20°S) have slightly higher values of HCl (dashed line in Figure 1), because of stronger $ClONO_2$ photolysis at these latitudes, combined with lower CH_4 (which increase formation of HCl via Cl + CH_4) and lower O_3 (which decreases the loss of Cl via Cl + O_3 and decreases the conversion of NO to NO_2 through NO + O_3). At these lower latitudes the relationships among CFC-11, N_2O, O_3, and CH_4 are different than at midlatitudes [*Plumb and Ko*, 1992], thus generating different tracer-tracer relationships, and through the indirect chemical effects outlined above, the HCl(CFC-11) relationship has also a different slope.

In the late fall of 1994 the measured HCl represents 60-75% of Cl_y at 20 km. The remaining 40-25% of inorganic chlorine is present as $ClONO_2$, ClO, and HOCl. ClO is observed at levels typically less than 5% of Cl_y. The concentration of HOCl can be calculated from its steady state relationship with observed concentrations of ClO and HO_2:

$$[HOCl^*] = k_{ClO+HO_2}[ClO][HO_2] / J_{HOCl} \quad (6)$$

The photolysis rate of HOCl (J_{HOCl}) and the reaction rate for ClO+HO_2 (k_{ClO+HO_2}) are calculated based on recommendations by *DeMore et al.* [1994]. Using equation (6), we calculated HOCl* to be less than 1% of the budget for the ER-2 altitude range. Because we do not have measurements of chlorine nitrate, we infer it from

$$[ClONO_2^*] = [Cl_y] - [HCl] - [ClO] - [HOCl^*] \quad (7)$$

for which we then derive a relation as a function of CFC-11 (see Figure 1 caption). Throughout this paper we will denote chemical species that are inferred from other in situ observations by an asterisk *. Total uncertainties of 70% and 80% are estimated for $ClONO_2^*$ and HOCl*, respectively, based on uncertainties in measurements and rate constants. The $ClONO_2$ calculated from its steady state relation with ClO and NO_2 is very close to $ClONO_2^*$ (C. R. Webster et al., manuscript submitted to Geophys. Res. Lett., "Evolution of HCl concentrations in the lower stratosphere from 1991 to 1996 following the eruption of Mt. Pinatubo", 1996)(hereinafter referred to as W96a).

These 1994 southern hemisphere measurements, where HCl is seen to be the dominant chlorine reservoir, are to be contrasted with those taken by the same instrument in the northern hemisphere between 1991 and 1993 [*Webster et al.*, 1994], which showed that HCl was measured to represent less than 40% of Cl_y. This change in chlorine partitioning could reflect the return of the lower stratosphere to low levels of aerosols 3 years after the eruption of Mount Pinatubo [W96a].

3.2. PSC Processing in Winter

By late fall, the vortex is well established [*Manney and Zurek*, 1993; *Schoeberl and Hartmann*, 1991] and minimum temperatures fall below 190 K. During the flight of August 6, 1994, the ER-2 attained a maximum latitude of 67.7°S before descending down to 15 km, climbing back to its cruise altitude of 19 km and returning to New Zealand. Observations of N_2O, wind speed, HCl, and ClO are shown in Plate 1, as a function of the latitude of the ER-2 aircraft. At most latitudes the observations of HCl closely follow the expected reference HCl (Plate 1 b). Poleward of 64°S, HCl abruptly decreases to very low values, while ClO increases to reach a maximum of about 0.9 ppbv. Comparing the HCl observations to the predicted reference

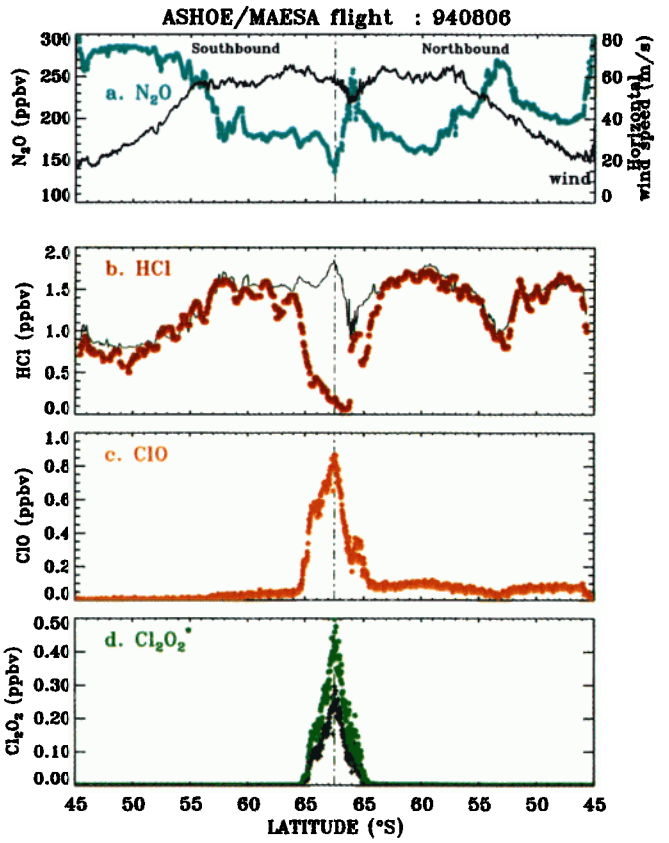

Plate 1. Flight of August 6, 1994: mixing ratios of (a) N_2O, (b) HCl, (c) ClO, (d) $Cl_2O_2^*$, calculated with $J_{Cl_2O_2}$ from *DeMore et al.* [1994] (black pluses) and $J_{Cl_2O_2}$ from *Huder and DeMore* [1995] (green dots), are plotted as a function of latitude. In Plate 1 a the solid line shows the horizontal wind speed. In Plate 1 b, the black line shows the empirically predicted unprocessed level of HCl (see Figure 1). The high values of N_2O on the first part of the southbound leg indicate the tropical origin of the air sampled there [*Tuck et al.*, 1995]. For this part of the flight we have therefore used the empirical HCl(CFC-11) relation typical of low latitudes (dashed line in Figure 1).

levels clearly shows that this decrease (by 90%) cannot be due to dynamical descent in the vortex. We therefore identify the observed loss of HCl and associated high values of ClO with recent chemical conversion.

At low temperatures and high ClO levels, a significant fraction of active chlorine can be present as Cl_2O_2, the ClO dimer [*Molina and Molina*, 1987; *Sander et al.*, 1989]. Assuming that Cl_2O_2 is in photochemical steady state equilibrium with the observed ClO, we can calculate it from the expression

$$[Cl_2O_2^*] = (k_{ClO+ClO}[ClO]^2)/(k_{Cl_2O_2+M}[M] + J_{Cl_2O_2}), \quad [8]$$

where M is a third body, N_2 or O_2, and $[M]$ thus represents the atmospheric density. The reaction rate constants for the ClO self-reaction ($k_{ClO+ClO}$) and the dimer thermal decomposition ($k_{Cl_2O_2+M}$) are taken from *DeMore et al.* [1994]. The dimer absorption cross sections are taken from the recent laboratory measurements by *Huder and DeMore* [1995]. The corresponding photolysis rate ($J_{Cl_2O_2}$) is calculated taking into account the albedo and overhead ozone variations along the ER-2 flight track [*Salawitch et al.*, 1994]. $Cl_2O_2^*$ determined in this manner has an

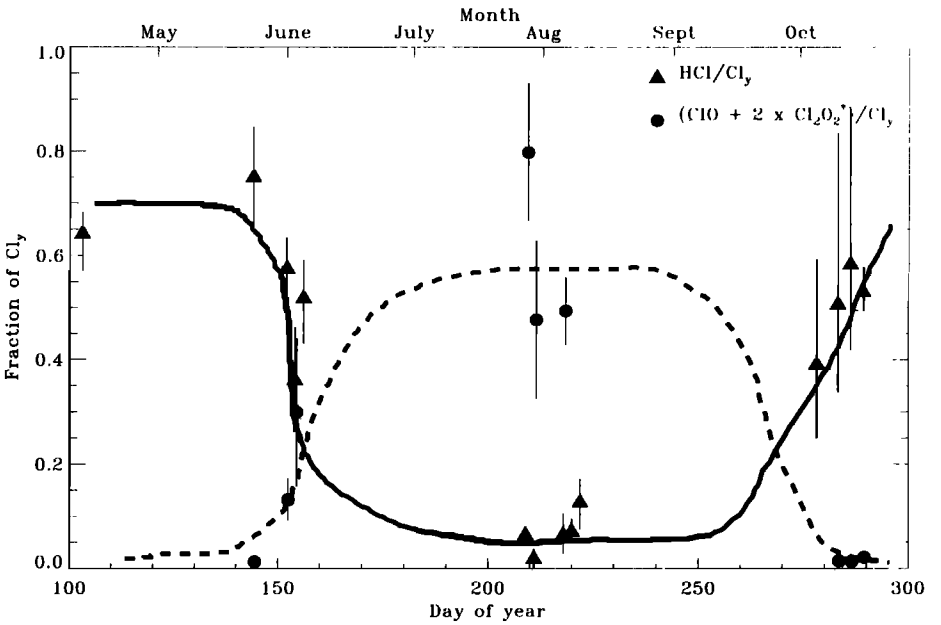

Figure 2. Time evolution of chlorine species inside the vortex between April and October 1994. The medians of observations are represented by the symbols (triangles, HCl/Cl_y; circles, $(ClO + 2\ Cl_2O_2)/Cl_y$) with their minimum and maximum, as the vertical bars. The points are selected for latitudes poleward of the maximum horizontal wind speed (typically south of ~ 64°S). The solid and dashed lines are visual guides passing through the HCl and ClO + 2 Cl_2O_2 observations.

uncertainty of about 80% [*Kawa et al.*, 1992]. At high solar zenith angles (> 83°) the steady state assumption no longer holds, and we have corrected $Cl_2O_2^*$ by the expected departure we derived from comparison with our time-dependent model. A similar approach is used to correct the steady state HOCl (for solar zenith angles > 85°). On the flight of August 6, 1994, Cl_2O_2 constitutes up to 0.5 ppbv, or 50% of the active chlorine (ClO + 2 Cl_2O_2 = 1.9 ppbv) at the peak ClO value.

Huder *et al.*'s new determination of the dimer cross sections yields a photolysis rate 40% lower than values calculated using currently recommended cross-sections [*DeMore et al.*, 1994]. Previous measurements seem to overestimate the cross section of Cl_2O_2 due to improperly accounted for contamination by Cl_2O. This has a large impact on our predicted steady state abundances of Cl_2O_2. As illustrated in Plate 1 d, $Cl_2O_2^*$ would be 40% lower if we used the cross sections by DeMore et al. Throughout this paper, we have adopted the recent absorption cross sections reported by *Huder and DeMore* [1995].

3.3. Evolution of HCl and ClO through the Vortex Lifetime

From measurements of HCl and ClO between April and October 1994, a picture of the evolution of inorganic chlorine partitioning at the inner edge of the vortex is built up before, during, and after the period when temperatures are cold enough for PSC formation. Figure 2 shows the observed time evolution of HCl/Cl_y and $(ClO + 2\ Cl_2O_2^*)/Cl_y$ inside the vortex during the ASHOE/MAESA campaign. We have selected observations obtained over 2°-3° latitude inside the vortex, the edge of which we define by the polar jet wind maximum as measured aboard the ER-2 [*Tuck et al.*, 1995, Table 1]. The release of active chlorine, ClO + 2 Cl_2O_2, mirrors the evolution of cold temperatures in the vortex. During the period between June and late August the temperatures are cold enough to promote the growth of PSCs whose surfaces provide sites for the heterogeneous reactions (1)-(3). The levels of HCl were first seen to decrease in early June 1994. By early August, HCl was extensively processed, and high levels of active chlorine were present inside the vortex. By October, photochemical recovery of HCl, through reaction (5), is nearly complete. On two occasions, October 10 and 13, the ER-2 sampled air where recovery of HCl to extremely high levels (HCl/Cl_y~1) had taken place in a low ozone environment (C.R. Webster et al., manuscript in preparation, "Total conversion of inorganic chlorine in polar stratospheric air severely depleted in O_3", 1996) (hereinafter referred to as W96b).

4. Stoichiometry of Chlorine Processing

Because of the 8-hour flight range of the ER-2, based in New Zealand, and the location of the PSCs well over Antarctica, flights during ASHOE/MAESA were confined mostly to the edge region of the Antarctic vortex. During two flights (July 28 and 30, 1994), however, the ER-2 flew through PSCs, and on several other occasions, it encountered air that had previously been exposed to temperatures below PSC formation thresholds (August 6, 8, and 10), as indicated by back trajectory calculations.

From observations obtained in the vortex prior to PSC processing, as shown in Figure 1, we have a knowledge of the expected unperturbed levels of HCl and $ClONO_2$. The difference between a measured mixing ratio for HCl and a reference value calculated from the simultaneously measured CFC-11 (or N_2O) represents the chemical loss, defined as follows:

$$\Delta HCl = HCl^*(CFC\text{-}11) - HCl. \quad (9)$$

We can use the same approach for $ClONO_2^*$, as inferred from the inorganic chlorine budget residual:

$$\Delta ClONO_2^* = ClONO_2^*(CFC\text{-}11) - ClONO_2^*. \quad (10)$$

$\Delta ClONO_2^*$ by itself does not bring any additional information as it depends on ΔHCl and ClO (according to our definitions in equations (10) and (7)). It is, however, a useful quantity to consider in parallel with ΔHCl, because it allows us to illustrate the behavior of both chlorine reservoirs at the same time.

By convention, and for simplicity, the sign in these expressions is such that for a net loss in HCl, ΔHCl is positive (the same applies for $ClONO_2^*$). *Webster et al.* [1993] demonstrated how the values of ΔHCl, $\Delta ClONO_2^*$, and $ClO + 2\ Cl_2O_2^*$ associated with each air parcel can give us information on the stoichiometry of PSC processing, since the net effect of heterogeneous reactions (1)-(3) is to increase ΔHCl, $\Delta ClONO_2^*$, and $ClO + 2\ Cl_2O_2^*$. Because of the large temperature dependence of heterogeneous reactions (1) - (3) the degree of chlorine activation depends on a balance between exposure time to cold temperatures and on the time spent in sunlight, which allows reformation of $ClONO_2$ [*Schoeberl et al.*, 1993].

Compact relationships between losses in chlorine reservoirs and production of reactive chlorine gases are seen for ASHOE/MAESA flights during the Antarctic winter. As we will show, these relationships are consistent with the stoichiometry of recent heterogeneous processing. Figure 3 presents ΔHCl and $\Delta ClONO_2^*$, as a functions of $ClO + 2\ Cl_2O_2^*$. All the mixing ratios have been normalized to Cl_y to account for variations in chlorine loading between air parcels (for a simple conversion to mixing ratios, the air parcels in the vortex generally contained 1.8-2.2 ppbv of inorganic chlorine). In early June 1994 (Figure 3 a), reactive chlorine accounted for up to 50% of Cl_y in the southern-most part of the flight, where HCl had been reduced by about 50%. Chlorine activation is more extensive at the end of July and in early August (Figure 3 b), where in some air masses, up to 90% of chlorine was in the form of reactive chlorine and little HCl was observed.

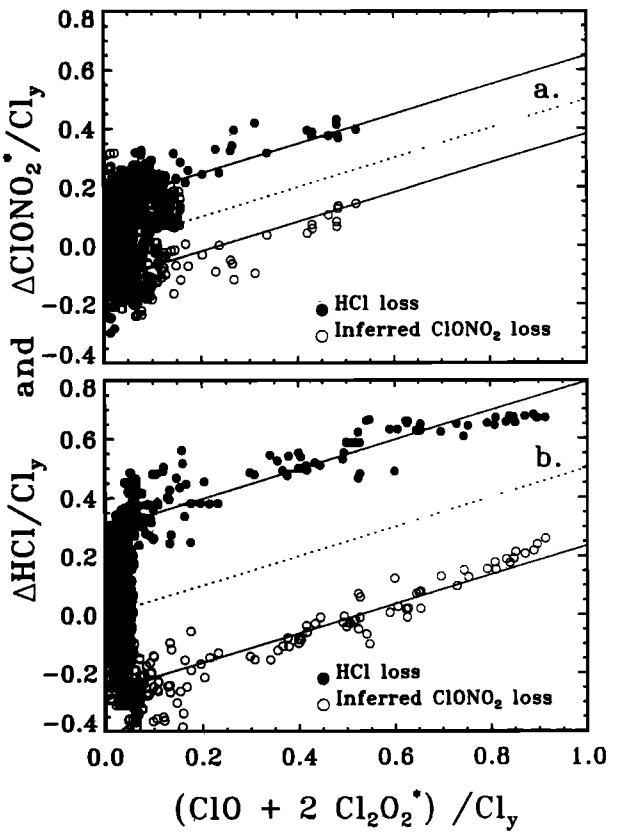

Figure 3. Loss of HCl (ΔHCl) and $ClONO_2^*$ ($\Delta ClONO_2^*$) as functions of reactive chlorine, $ClO + 2\ Cl_2O_2^*$. All these quantities have been normalized to the total inorganic chlorine Cl_y. ASHOE/MAESA flights of (a) June 1 and 3, 1994, (b) July 28, and August 6, 1994. Observations corresponding to N_2O values greater than 260 ppbv, and pressures above 70 mbar have been excluded from these figures. The dashed line has a slope of 1:2. The two solid lines correspond to slopes of 1:2 going through the observations for $(ClO + 2\ Cl_2O_2^*)/Cl_y > 0.2$.

Simultaneous measurements of HCl and ClO were previously made in the Arctic vortex aboard the ER-2 [*Webster et al.*, 1993; *Toohey et al.*, 1993] during the Airborne Arctic Stratospheric Experiment II (AASE II) campaign. In their analysis of the AASE II observations, *Webster et al.* [1993] saw a striking 1:2 slope for the correlation between ΔHCl and $ClO + 2\ Cl_2O_2^*$ corresponding to the stoichiometry of the heterogeneous reaction (1), by which one HCl is converted to one Cl_2, as depicted in Figure 4 a for the AASE II flights of December 12, 1991, and January 20, 1992. For the highest values of active chlorine, the observations of HCl and inferred $ClONO_2$ depart from the 1:2 slope. This departure was not seen as clearly in Webster et al. and is caused here by the use of Cl_2O_2 cross sections based on *Huder and DeMore* [1995] (instead of *Burkholder et al.* [1990]), which results in enhanced $Cl_2O_2^*$, as discussed in section 3.1. $ClO + 2\ Cl_2O_2^*$ exceeds Cl_y for some points inside the vortex, but one has to keep in mind that the total uncertainty in $ClO + 2\ Cl_2O_2^*$ is close to 50%.

For ASHOE/MAESA flights the slope of the correlation is close to 1:2, providing further evidence for the occurrence of reaction (1). However, there is a vertical offset. In other words, $\Delta HCl > 1/2\ (ClO + 2\ Cl_2O_2)$. The points that fall on the parallel 1:2 lines correspond to latitudes poleward of 64°S. The offset (or the non zero y intercept) reflects a net gain of $ClONO_2$ and loss of HCl compared with the relationships derived from observations in the fall.

Pure photochemical relaxation of the $HCl/ClONO_2$ ratio could occur as a response to the decreased amount of sunlight as the vortex goes from fall to winter. From time-dependent photochemical calculations we evaluate that this effect could generate a decrease of 70 pptv/month for HCl in the edge region of the vortex, accounting for up to a third of the observed offset. As discussed in section 3.1, the air that was sampled by the ER-2 in early June and late July could be air that originated from a higher altitude inside the vortex and as a result was not seen by the ER-2 in the fall. However, profiles of HCl obtained by HALOE in the fall of 1994 show that inside the vortex the HCl/Cl_y ratio is fairly constant in the 20-30 km region at 70% (J. Russell, personal communication, 1996). Thus the decrease in HCl/Cl_y could not be caused by descent. Finally, cold temperatures below 200 K are pervasive in fall/winter high latitudes, and heterogeneous reactions on sulfate aerosols could have partially converted HCl to Cl_x. With sufficient sunlight, some of the reactive chlorine in turn could have been converted back to $ClONO_2$, thus changing the partitioning between HCl and $ClONO_2$. The succession of reactions taking place can be summarized as follows

$$HCl + ClONO_2 \rightarrow Cl_2 + HNO_3 \quad (1)$$

$$Cl_2 + h\nu \rightarrow 2\,Cl \quad (11)$$

$$2\{\, Cl + O_3 \rightarrow ClO + O_2 \,\} \quad (12)$$

$$2\{\, HNO_3 + h\nu \rightarrow NO_2 + OH \,\} \quad (13)$$

$$2\{\, ClO + NO_2 + M \rightarrow ClONO_2 + M \,\} \quad (4)$$

$$HCl + ClONO_2 + 2\,O_3 + HNO_3 \rightarrow 2ClONO_2 + 2\,O_2 + 2\,OH. \quad (14)$$

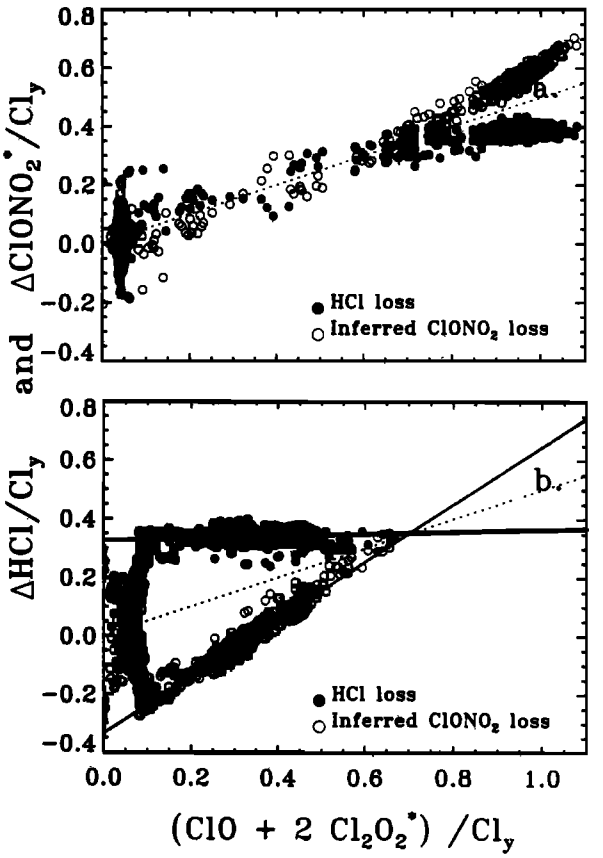

Figure 4. Same as for Figure 3, but for AASE II flights of (a) December 12, 1991, and January 20, 1992, (b) February 13 and 17, 1992.

We estimate that 5-6 exposures to temperatures in the 197-199 K range for a few hours at a time would be enough to account for a decrease in HCl by a few tenths of ppbv (and increase $ClONO_2$ by twice that amount), due to heterogeneous reaction (1) on sulfate aerosols followed by excursions to lower latitudes. In this manner a large part of the offset can be attributed to prior processing of chlorine reservoirs on background sulfate aerosols or on PSCs. Thus while the 1:2 slope in Figure 3 comes from the stoichiometry of (1), the y intercept can be interpreted as the extent of past PSC processing, or the "memory" of chlorine activation through (1) for HCl. $ClONO_2$ on the other hand can recover through (4), resulting in the net stoichiometry of (14). As noted above, the AASE II data do not show such a non zero y intercept. This would suggest that the processed air encountered had been exposed to only one PSC event in the Artic vortex, where PSCs are not as extensively present as in the Antarctic.

The compactness of the slopes in Figures 3 and 4 indicate that the process of activation/deactivation is very similar for all the air parcels sampled and that their temperature histories followed fairly similar evolutions for each individual flight. This is what we would expect, as the ER-2 flight tracks during ASHOE/MAESA were usually designed to follow potential temperature surfaces. Under adiabatic conditions, air is transported along such surfaces of constant potential temperature. In the following, we interpret the patterns in Figures 3 and 4 by separating them into four cases reflecting different temperature history regimes:

4.1. On going Processing: $\Delta HCl = 1/2(ClO + 2\ Cl_2O_2)$

Reaction (1) dominates the conversion process and yields a 1:2 net stoichiometry, in which one HCl is converted to one Cl_2 (which is then rapidly converted to 2 ($ClO + 2\ Cl_2O_2$)). The AASE II flights of December 12, 1991, and January 20, 1992, fall into this category (Figure 4 a) [*Webster et al.*, 1993].

4.2. Recovery of $ClONO_2$: ΔHCl = Constant

Following event 4.1., if there is sufficient sunlight, NO_2 is produced from HNO_3 decomposition (photolysis and reaction with OH) and reacts with ClO to form chlorine nitrate. Thus $ClONO_2$ increases and $\Delta ClONO_2$ decreases linearly with reactive chlorine, with a slope of 1, following the stoichiometry of (4). This can be seen during the AASE II flights of February 13 and 17, 1992. HCl recovers much more slowly, as indicated by the small slope of ΔHCl in Figure 4 b.

4.3. Multiple Processing: $\Delta HCl = 1/2(ClO + 2\ Cl_2O_2) + c$

At the edge of the Antarctic vortex, temperatures are cold enough for multiple processing events to take place, interrupted by excursions into sunlight that allow partial recovery of $ClONO_2$. Events 4.1. and 4.2. can follow each other several times until all of HCl has been consumed. The ASHOE/MAESA flights in Figure 3 show a 1:2 slope with a y intercept of 20-30% Cl_y, implying that the accumulated effect of 4.1. and 4.2. could have been to convert a fraction of Cl_y back to $ClONO_2$, through the net reaction (14). (From our discussion above, a third of that offset could be due to pure gas phase repartitioning at high latitudes.)

4.4. Low HCl Levels: ΔHCl = Constant

When most of HCl has been consumed, the rate for (1) becomes very slow. At cold enough temperatures, $ClONO_2$ can be directly converted to HOCl through (2) on sulfate aerosols or type II PSCs (this reaction is ineffective on NAT; see Figure 5). Such a case would be translated into a slope of 1:1 for $\Delta ClONO_2$ and of zero for ΔHCl. In Figure 3 b and 4 b, ΔHCl is seen to depart from the 1:2 line for high ($ClO + 2\ Cl_2O_2$)/Cl_y values, possibly indicating the occurence of (2). However, these changes in slopes have to be interpreted cautiously given all the uncertainties associated with the HCl/CFC-11 relationship and the photolysis rate calculations at high solar zenith angle (SZA). Note that without temperature history consideration and knowledge of the type of PSC formed, we cannot a priori distinguish between cases 4.2 and 4.4 .

From these observations it seems that even though processing begins with more HCl than $ClONO_2$, partial recovery of $ClONO_2$ through the net reaction (14) allows near complete heterogeneous loss of HCl. Interestingly, this would suggest that the conversion to active chlorine is HCl-limited in the edge region of the Antarctic vortex. Excursions of air parcels to lower latitudes provide enough sunlight to produce NO_x, which combines with ClO (via reaction (4)) to produce small amounts of $ClONO_2$. Similarly, production of HO_x at lower latitudes results in small amounts of HOCl (via $ClO + HO_2$). Subsequently, as the parcel returns to higher latitudes and colder temperatures, heterogeneous reactions of HCl with both reservoirs via (1) and (3) continue to deplete HCl [*Jaeglé*, 1996].

In this manner, reaction (1) is responsible for the rapid early winter loss of HCl, until all of $ClONO_2$ has been consumed. Reactions (1) and (3) then combine to continue this process, at a

slower rate, limited by excursions into sunlight. Thus the near-total removal of HCl that was observed in this study and in airborne column measurements [*Toon et al.*, 1989] can take place from excursions in and out of sunlight, with a resupply of HOCl and $ClONO_2$, which provide oxidation partners for HCl. Deeper inside the vortex it has been suggested that HO_x and NO_x production by galactic cosmic rays [*Müller and Crutzen*, 1993] could replace the role of these excursions in generating total loss of HCl [*Liu et al.*, 1992] via (1) and (3).

The high amounts of $ClONO_2$, inferred here, form the so-called chlorine nitrate "collar," first discovered in ground-based measurements [*Farmer et al.*, 1987] and remote soundings from aircraft [*Toon et al.*, 1989] in the springtime Antarctic and, subsequently, measured in the Arctic [*von Clarmann et al.*, 1993; *Toon et al.*, 1994; *Oelhaf et al.*, 1994]. Observations aboard the UARS satellite have revealed a global picture of this collar which surrounds the Antarctic vortex between 50° and 60°S and is present from July to September [*Roche et al.*, 1993, 1994].

5. Photochemical Model Along Trajectories

To better understand the mechanisms responsible for the repartitioning of chlorine species during the polar winter, we use a Lagrangian photochemical model along trajectories [*Nair*, 1996] adapted from the Caltech-JPL model. The model includes 50 species in the NO_y, Cl_y, Br_y, HO_x and O_x families. A full methane oxidation scheme is included. Close to 200 gas phase reactions, 50 photolytic reactions, and 6 heterogeneous reactions on various surfaces are used. Most reaction rates are based on the compilation by *DeMore et al.* [1994]. Absorption cross sections are also taken from DeMore et al., except for HOBr and Cl_2O_2, for which more recent laboratory measurements by *Rattigan et al.* [1996] and *Huder and DeMore* [1995] are used. The photolysis rates are calculated using climatological ozone profiles scaled to total ozone mapping spectrometer (TOMS) overhead ozone corresponding to the end point of the trajectory.

The main heterogeneous reactions and their uptake probabilities, corresponding to different types of surfaces adopted in this work, are listed in Table 2. Figure 5 illustrates the temperature dependence of the three most important heterogeneous reactions (1) to (3) for different surface types. Recently, the high reactivity of bromine compounds on heterogeneous surfaces has been observed in the laboratory [*Hanson and Ravishankara*, 1995; *Abbatt*, 1994]. In addition to the hydrolysis of bromine nitrate (Table 2) we have included other possible heterogeneous bromine reactions, such as HCl + HOBr and HBr + HOCl, and found that their effect was to slightly increase chlorine activation. This effect was minor, however, compared with reactions (1)-(3), as was shown by *Lary et al.* [1995] and *Danilin et al.* [1995b].

Elucidating the exact phase and composition of the PSC particles is not in the scope of this work and is addressed elsewhere [*Del Negro et al.*, this issue; *Dye et al.*, 1996]. Instead, we use simplified assumptions for each flight examined, based on the observed surface area and composition of the aerosols. Many uncertainties still remain on the early phase of the formation and growth mechanism of polar stratospheric clouds, which can be characterized as type I or type II PSCs. The possible composition of type I PSCs include nitric acid trihydrate (NAT), nitric acid dihydrate (NAD), supercooled H_2O-HNO_3, supercooled ternary solutions (STS) $HNO_3/H_2SO_4/H_2O$, and sulfuric acid tetrahydrate (SAT) [*Hanson and Mauersberger*, 1988; *Wornsop et al.*, 1993; *Tabazadeh et al.*, 1994; *Molina et al.*, 1993; *Zhang et al.*, 1993]. Type II PSCs are composed of water ice [*Steele et al.*, 1983].

In the model the composition and volume growth of supercooled ternary solution is obtained according to the formulation of *Carslaw et al.* [1995], and we assume heterogeneous reactions on STS to take place with the same reactivities as on sulfate aerosols. The presence of NAT particles is predicted as a function of H_2O and HNO_3 local partial pressures, using the saturation vapor pressures given by *Hanson and Mauersberger* [1988]. The corresponding surface area is calculated from the amount of condensed species using a specified radius of 1 μm. Similarly, ice particles are predicted as a function of H_2O partial pressure, with the saturation vapor pressure given by *Marti and Mauersberger* [1993]. For these generally larger particles, we assume a 10 μm radius to calculate the surface area. Condensed species are returned to the gas phase when the clouds evaporate. An example of calculated growths of STS and NAT and ice PSCs as a function of temperature is shown in Figure 6.

We do not consider the effects of denitrification in this study, because it was generally not observed for the air masses sampled during ASHOE/MAESA [*Keim et al.*, this issue]. However, the formation of NAT in the model temporarily sequesters HNO_3 in the solid phase and thus can effectively slow the recovery of $ClONO_2$.

Unless otherwise specified, H_2O, CH_4, and O_3 are kept fixed at their measured values. If no measurements are available for a particular flight, these species are obtained from empirical tracers

Table 2. List of Heterogeneous Reaction Probabilities

	Reaction				Surface type			
					H_2SO_4	NAT	SAT	Ice
(1)	$ClONO_2$	+ HCl	$\rightarrow Cl_2$	+ HNO_3	(b)	(d)	(d)	0.2 (a)
(2)	$ClONO_2$	+ H_2O	$\rightarrow$ HOCl	+ HNO_3	(b)	0.001 (a)	(e)	0.1 (a)
(3)	HOCl	+ HCl	$\rightarrow Cl_2$	+ H_2O	(c)	(f)	= NAT	0.3 (a)
(4')	N_2O_5	+ H_2O	$\rightarrow$ 2HNO_3		0.1 (a)	0.0003 (a)		0.1 (a)
(5')	$BrONO_2$	+ H_2O	$\rightarrow$ HOBr	+ HNO_3	0.5 (g)	0.006 (h)	=NAT	0.3 (a)
(6')	N_2O_5	+ HCl	$\rightarrow ClNO_2$	+ HNO_3		0.003 (a)		0.03 (a)

(a) *DeMore et al.* [1994]; (b) *Hanson and Ravishankara* [1994]; (c) *Hanson et al.* [1994], (d) *Hanson and Ravishankara* [1993]; (e) *Zhang et al* [1993]; (f) *Abbatt and Molina* [1992]; (g) *Hanson and Ravishankara* [1995]; (h) *Lary et al* [1996]

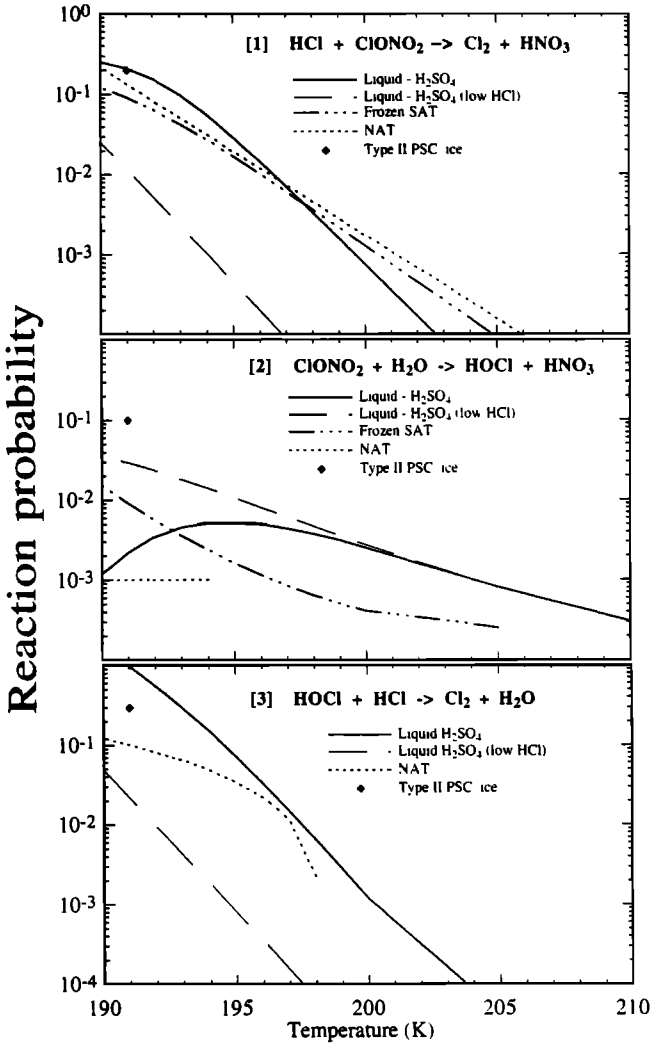

Figure 5. Heterogeneous reaction probabilities as a function of temperature on sulfuric acid (line, H_2SO_4), sulfuric acid tetrahydrate (dashed-dotted, SAT), nitric acid tetrahydrate (short dashed, NAT), and ice (diamonds) for reactions (1) HCl + $ClONO_2 \rightarrow Cl_2 + HNO_3$, (2) $ClONO_2 + H_2O \rightarrow HOCl + HNO_3$, and (3) $HOCl + HCl \rightarrow Cl_2 + H_2O$. The dependence on HCl levels is shown for reactivities on sulfuric acid (long dashed, low HCl = 0.01 ppbv)

relationships inferred from other flights. Total nitrogen (NO_y), chlorine (Cl_y), and bromine (Br_y) are conserved during the calculation. NO_y is specified from in situ observations, and Cl_y is based on in situ CFC observations. The levels of inorganic bromine (Br_y) used in our analysis are based on whole air sampler measurements of organic bromine during AASE II [*Schauffler et al.*, 1993], adjusted to account for the increase in bromine since 1992 and the in situ observations of BrO during ASHOE/MAESA (R. M. Stimpfle et al., manuscript in preparation, 1996). Whenever possible, initial conditions are taken from observational data. Initialization of most other species is obtained from steady state conditions at the latitude of the end point of the calculations.

To investigate the impact of the temperature and latitude history of the air parcels encountered by the ER-2, we couple the photochemical model with 10-day trajectory calculations. Daily analysis of wind and temperatures obtained from the European Centre for Medium-range Weather Forecasts (ECMWF) were used to calculate three-dimensional back trajectories [*Tuck et al.*, 1995]. Latitude, longitude, pressure, and temperature once derived are used as input to the photochemical model which is run forward along the trajectory, with a time step varying between 30 min and 1 min.

One has to keep in mind the major uncertainties associated with photochemical Lagrangian calculations in the polar environment. The main factors influencing these calculations include (1) uncertainties in how well temperatures along a 10-day back trajectory can be known, (2) the choice of initial conditions for chlorine partitioning, and (3) assumptions concerning the phase of PSCs formed. Throughout the analysis presented here, we address these issues by using different assumptions for points (2) and (3). While a generally high level of confidence is associated with temperature histories for the first 3-4 days of the back trajectories, uncertainties increase rapidly afterward. Whenever our results critically depend on the exact temperature history, we attempt to assess the level of this dependence by comparing ECMWF trajectories with Goddard Space Flight Center (GSFC) isentropic trajectories obtained from NMC (National Meteorological Center) wind and temperature analysis [*Schoeberl et al.*, 1992].

In a study of the organic and inorganic chlorine budget measured by the balloon-borne MkIV instrument [*Toon et al.*, 1991], comparison between measured and expected chlorine levels has led to making a case for a missing inorganic chlorine species - namely, $HClO_4$ produced by uptake of ClO on volcanic sulfate aerosols [*Jaeglé et al.*, 1996]. The effect of this new species would be to temporarily reduce the inorganic chlorine available for HCl formation, and might explain the low levels of HCl observed by the ALIAS instrument during the 2 years following Mt. Pinatubo's eruption (W96a). Whether this mechanism could take place in the winter polar regions, where high ClO concentrations and large surface areas provided by polar stratospheric cloud (PSC) particles coexist, is an interesting issue to consider. The uptake coefficients for ClO on ice and NAT surfaces [*Kenner et al.*, 1993] are too slow to be of

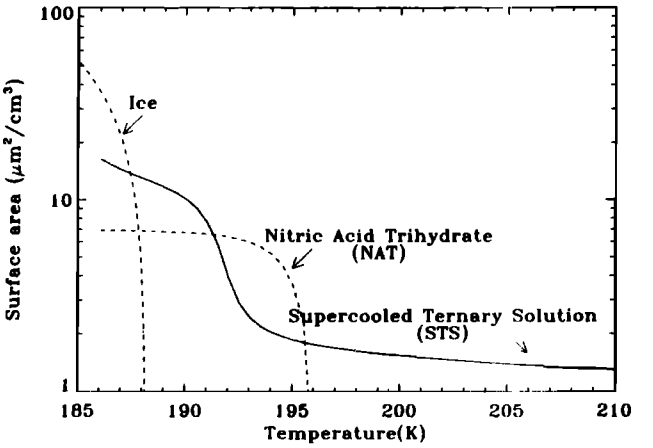

Figure 6. Model-calculated aerosol surface area growth as a function of temperature. Supercooled ternary solution (line, formulation of *Carslaw et al.*, [1995]), nitric acid trihydrate (short dashed, with assumed radius = 1 μm), and ice (dashed dotted, with assumed radius = 10 μm) surface areas as a function of temperature. Conditions used: p = 55 mbar, H_2O = 5 ppmv, HNO_3 = 10 ppbv, H_2SO_4 = 0.5 ppbv.

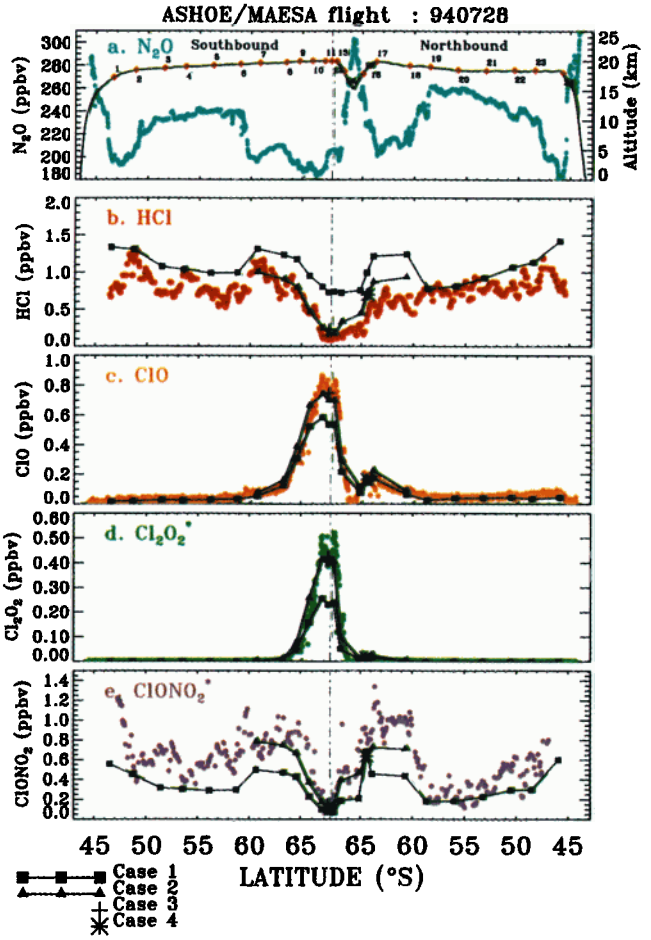

Plate 2 a. Flight of July 28, 1994. Comparison between observations and results from 10-day photochemical trajectory calculation for chlorine species, (b) HCl, (c) ClO, (d) Cl_2O_2*, (e) $ClONO_2$*. All species with stars are calculated from observations assuming steady state (see text). N_2O and altitude are represented in the top panel as well as the specific air parcel locations used in the analysis. The model results assume heterogeneous reactions on background sulfate aerosols and growth of supercooled ternary solutions (STS) particles as a function of temperature (see Figure 6). The solid squares connected with lines (case 1) represent model calculations at the end of the 10-day trajectory assuming no previous processing of chlorine, while the triangles (case 2) show the model results assuming an initialization with 0.35 ppbv of HCl (or 20% of Cl_y) having been previously heterogeneously processed. The plus at 67°S (case 3) and the star at 64°S (case 4) correspond to model cases assuming, formation of types I and II PSCs, and frozen SAT particles (see text), respectively. The vertical line going through all the panels indicates the southern most latitude reached (~ 67.5°S).

significance. Recent measurements of ClO uptake on sulfuric acid [*Abbatt*, 1996] indicate that this reaction would be too slow to compete with the other heterogeneous reactions. For this reason we have not included considerations of missing chemistry in this study.

In the following two sections we examine whether the model simulations can account for the observed amounts of HCl lost and ClO produced as a result of a PSC encounter. In particular, we pose the question of whether different aerosol surfaces and temperature histories leave specific fingerprints on the partitioning of chlorine species and other reactive species. To that end we focus on a detailed analysis of two ER-2 flights made on July 28, 1994, and August 6, 1994. During this period of austral winter, temperatures are generally very cold throughout the vortex. Intense heterogeneous processing has been taking place since early June [*Waters et al.*, 1993; *Santee et al.*, 1994].

6. On going Heterogeneous Processing: July 28

Observations obtained during the flight of July 28, 1994, are shown in Plates 2 a and 2 b, as a function of latitude. During this flight, temperatures as cold as 190 K were measured southward of 60°S (top panel in Plate 2 b), and the ER-2 flew through a polar stratospheric cloud between 65.5° and 67.5°S. Ten-day back trajectories show that the air had been rapidly cooling over the 12 hours prior to being sampled by the ER-2 (Figure 7 a). Inside the vortex (the maximum horizontal wind was observed at 64°S), ClO mixing ratios reached a maximum of 0.85 ppbv, while HCl levels decreased to values lower than 0.2 ppbv (Plate 2 a), close to the detection limit of the instrument.

6.1. Model Results along Trajectories

In a first step we assume in our calculations that the aerosols are in the liquid phase and that they grow by condensation of

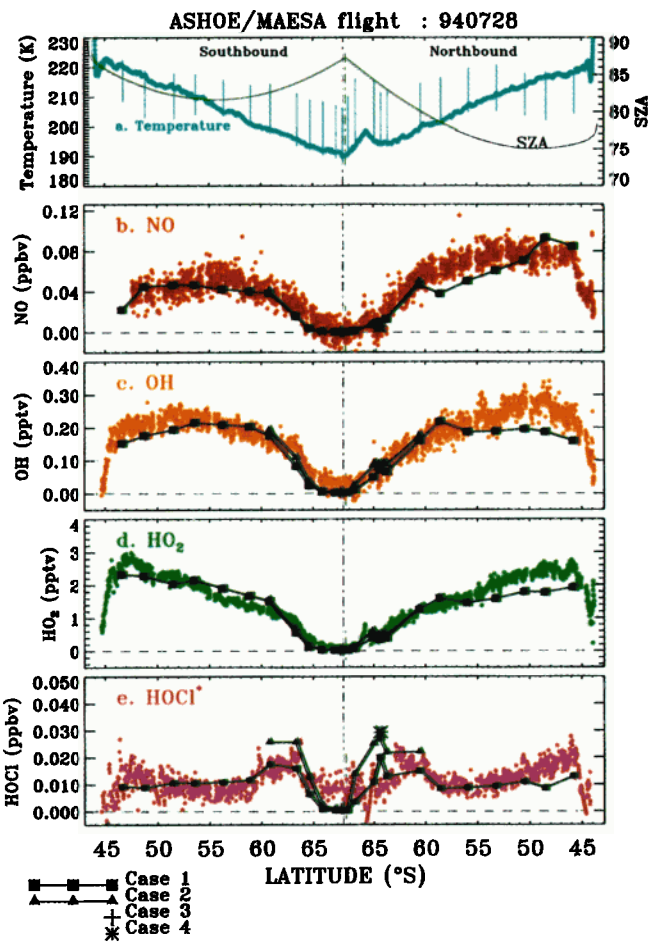

Plate 2 b. Same as for Plate 2 a but for (b) NO, (c) OH, (d) HO_2, and (e) HOCl*. Temperature and solar zenith angle along the ER-2 flight track are presented in the top panel. The vertical bars show the range of temperatures encountered in the previous 10 days, as obtained from back trajectory calculations.

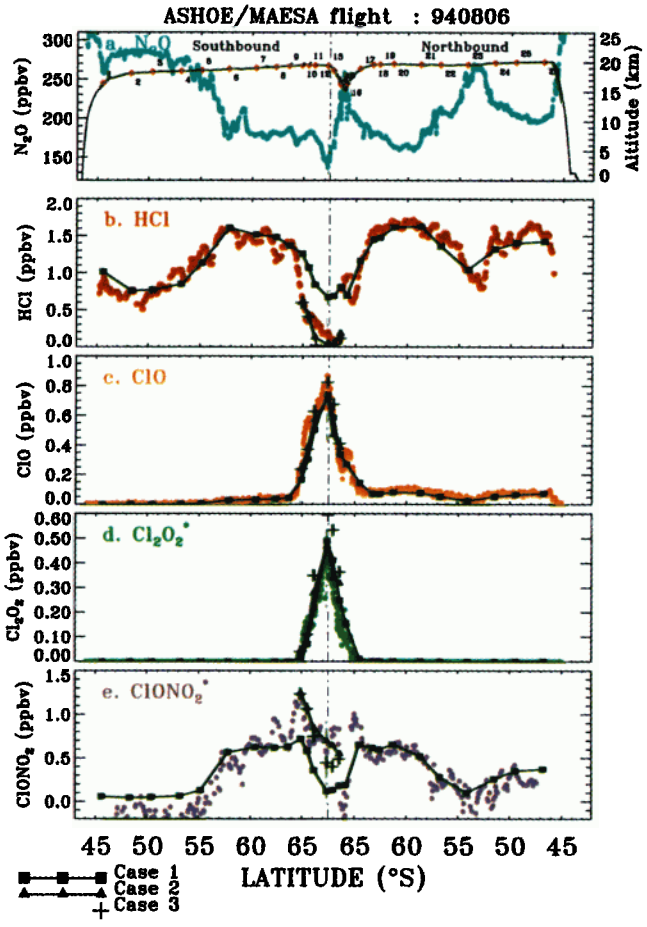

Plate 3 a. Flight of August 6, 1994. Same as Plate 2 a. The solid squares connected with lines (case 1) represent model calculations assuming no previous processing of chlorine, while the triangles (case 2) show the model results assuming that 0.35 ppbv of HCl have been heterogeneously processed. Both cases assume heterogeneous reactions on sulfate aerosols and STS. The plus symbols (case 3) show model results assuming pre processing and formation of NAT and ice PSCs.

HNO_3 and H_2O to form supercooled ternary solutions (STS) at low temperatures. The levels of HCl, ClO, Cl_2O_2*, and $ClONO_2$* are compared to the end points of the back trajectory calculations in Plate 2 a, as a function of latitude. Two different sets of model initializations are considered. In case 1 (squares) we assume no pre processing of the chlorine reservoirs: HCl and $ClONO_2$ are initialized from their empirical relations with CFC-11 in the fall (see section 3.1), which in the vortex yield a ratio of 70% HCl to 30% $ClONO_2$. In the second case (case 2, triangles) we assume that poleward of 61°S (1) 0.35 ppbv of HCl and $ClONO_2$ (~15 % of Cl_y) had previously undergone heterogeneous processing and that (2) $ClONO_2$ has had time to recover (thus forming 45% of Cl_y), such that ClO levels were back to low values, and HCl remains at its depleted levels (~55% of Cl_y). This initialization is consistent with observations in early June (Figure 3 a) and our stoichiometry analysis in section 4. As shown in Plate 2 a, the first case clearly overestimates HCl poleward of 66°S and underestimates ClO, suggesting that HCl had indeed been processed earlier than 10 days before. If we assume no previous processing, then the maximum amount of active chlorine liberated is limited by the smallest reservoir, which is $ClONO_2$ in case 1. Previous processing of HCl followed by conversion of ClO into $ClONO_2$ (case 2) results in higher predicted levels of ClO and an extremely well reproduced sharp latitudinal gradient in ClO (Plate 2 a, panel c).

Note that observations of HCl outside the vortex on the southbound leg are lower than our derived 'unperturbed levels', but are within the uncertainty of HCl for this particular flight, for which optical fringes resulted in uncertainties as large as ± 0.2 ppbv. It is also possible that his high-latitude air could have been exposed to sustained low temperatures such that heterogeneous chemistry on background sulfate aerosols could have slowly depleted HCl over a time period of a month or two [*Hanson et al.*, 1994].

The NO mixing ratios (Plate 2 b) are decreasing southward of 57°S due to the slow photolysis of HNO_3 at higher latitudes combined with heterogeneous conversion of N_2O_5 on sulfate aerosols [*Fahey et al.*, 1993; *Gao et al.*, 1997]. South of 66°S, extremely low levels of NO are observed: high concentrations of ClO rapidly convert NO_x to $ClONO_2$. The latitudinal gradient in NO is well reproduced, in particular the near-zero values inside the vortex.

Odd-hydrogen (HO_x) mixing ratios predicted by the model follow the shape of OH and HO_2 in situ observations as a function of latitude (Plate 2 b) and are generally within the uncertainty of the measurements (± 30%). Our calculation includes $BrONO_2$ hydrolysis with a sticking coefficient of 0.5

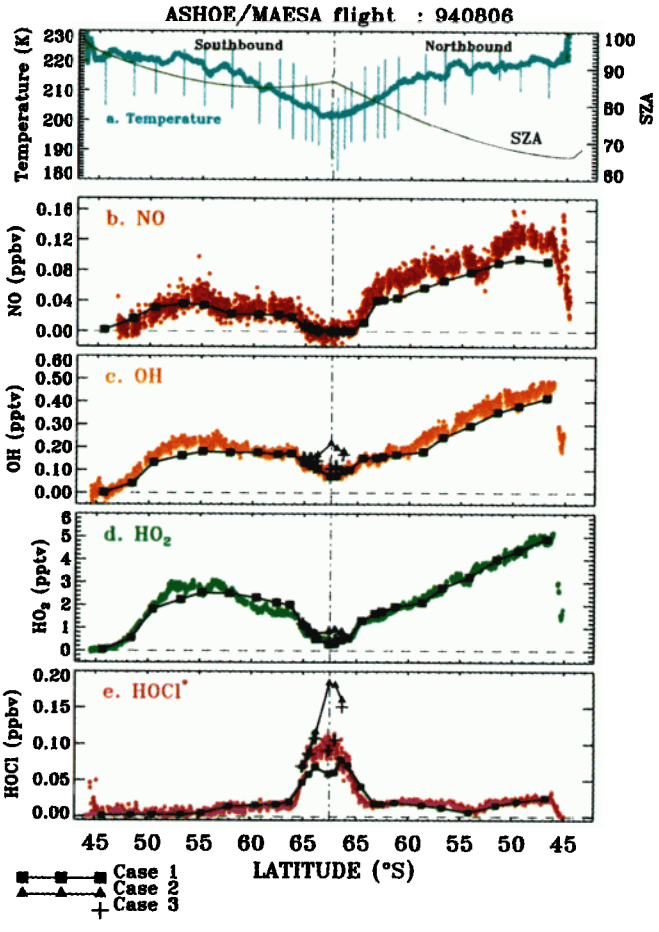

Plate 3 b. Flight of August 6, 1994. Same as Plate 3 a, but for (a) temperature and altitude, (b) NO, (c) OH, (d) HO_2, and (e) HOCl*.

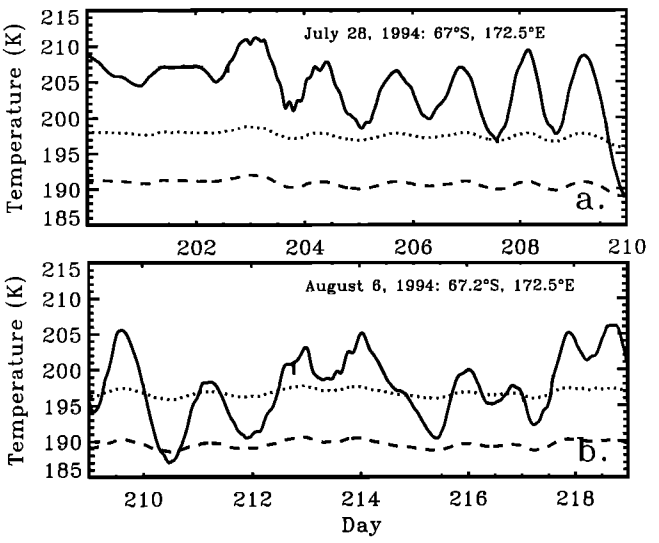

Figure 7. Back trajectory temperatures for end points on (a) July 28, 1994, at 67°S, 172.5°E (parcel 11 in Plate 2 a); and (b) August 6, 1994, at 67.2°S, 172.5°E (parcel 12 in Plate 3 a). The dotted lines show the NAT formation temperatures, T_{NAT} [*Hanson and Mauersberger*, 1988], for (a) 7.2 ppbv HNO_3 and 4.8 ppmv H_2O; (b) 10.3 ppbv HNO_3 and 5 ppmv H_2O. The dashed line corresponds to the ice formation temperature T_{ICE}. The variations in both T_{NAT} and T_{ICE} reflect the changes in pressure along the trajectories.

[*Hanson and Ravishankara*, 1995]. As discussed by *Hanson and Ravishankara* [1995] and *Lary et al.* [1995], $BrONO_2$ hydrolysis on sulfate aerosols leads to increased HOBr levels, which via photolysis produces higher levels of HO_x, especially close to sunrise. Not including $BrONO_2$ hydrolysis in our calculations would result in HO_x values 20% lower at a SZA of 75° and 65% lower at a SZA of 85°.

If we now study parcel 11 of Plate 2 a, with a temperature history shown in Figure 7 a, we obtain model calculations for the evolution of individual species during the 10 days prior to the ER-2 measurement, as shown in Figure 8. These results correspond to the initialization in case 2, assuming pre processing of HCl. When the temperature decreases below 200 K (on day 207.5), the reaction of HCl and $ClONO_2$ on STS becomes fast enough to deplete slightly both chlorine reservoirs and to increase Cl_x.

The precipitous drop in temperatures for the last 12 hours of the trajectory causes the reactivity of (1) to increase by an order of magnitude, while at the same time, the uptake of HNO_3 generates the growth of aerosols (Figure 6) to form supercooled ternary solutions. As a consequence of high reactivity and increased surface area, HCl and $ClONO_2$ are rapidly converted to Cl_2 (through reaction (1)) which itself is transformed to ClO and Cl_2O_2. Heterogeneous reactions of HCl with HOCl (reaction (3)) and of $ClONO_2$ with H_2O (reaction (2)) result in less than 0.02 ppbv of additional ClO production. Model-calculated HCl, $ClONO_2$, ClO, Cl_2O_2 compare very well with the observed and

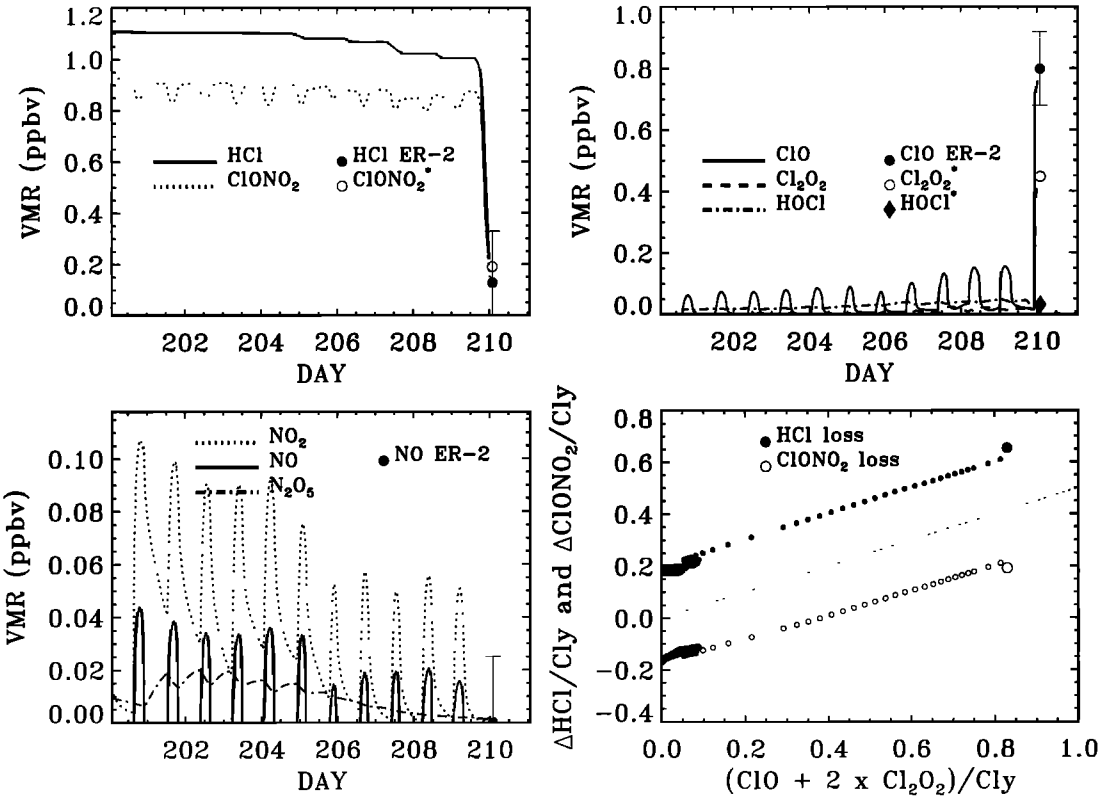

Figure 8. Evolution of model calculations along a trajectory starting July 18 (day 200) and ending July 28, 1994 (67°S, 172.5°E, at 22:34 UT). Parcel 11 in Plate 2 a. Values of the species as observed by the ER-2 are represented by the symbols with error bars at the end of the trajectory. Temperatures along the trajectory are shown in Figure 7 a.

derived quantities at the intercept of the trajectory with the ER-2 flight track. The high levels of ClO suppress NO_x via reaction of ClO and NO_2 to form $ClONO_2$. Indeed, the NO levels are below the detection limit of the instrument.

The analysis we presented in section 4 showed that the stoichiometry of the reaction converting HCl and $ClONO_2$ to active chlorine is 1:2, suggesting a dominant role for $ClONO_2+HCl \rightarrow Cl_2+HNO_3$. In our model simulations, where heterogeneous reactions with laboratory measured reaction rates are included, we see the same behavior as illustrated in the bottom right-hand panel of Figure 8, where we plot the loss in HCl as a function of model-produced active chlorine over the course of the 10-day trajectory. Thus, as expected, the overall stoichiometry of the heterogeneous reactions listed in Table 2 is close to that of reaction (1).

The bottom right-hand panel in Figure 8 illustrates the evolution of reservoir losses and active chlorine production for a given air parcel as a function of time rather than an instantaneous snapshot for many air parcels as in Figure 3 and 4. The slopes of these figures are similar because they show, in one case, the changes in HCl and $ClONO_2$ for a given moment in a suite of parcels that have experienced cold temperatures for different lengths of time (Figure 3 and 4), and in the other case, the time evolution of HCl and $ClONO_2$ in a parcel as it encircles the pole, steadily increasing the length of time exposure to cold temperatures (Figure 8).

6.2. Heterogeneous Reaction $HOCl + HCl \rightarrow Cl_2 + H_2O$

When temperatures fall below 198 K, reaction (3) begins to be important and HOCl rapidly reacts with HCl to produce Cl_2 (see Figure 5). HOCl itself is mainly formed by the reaction $ClO + HO_2 \rightarrow HOCl + O_2$ as well as heterogeneously via (2) (which contributes to up to 40% of HOCl production under the July 28 conditions). In this manner, as pointed out by *Prather* [1992] and *Crutzen et al.* [1992], reaction (3) acts as an effective sink for HO_x in the polar stratosphere. HO_x observations inside the vortex during ASHOE/MAESA provide direct evidence for reaction (3) (also see K96): panels c and d in Plate 2 b illustrate how levels of OH and HO_2 are indeed suppressed inside the vortex, with mixing ratios of ~0.025 (±0.01) pptv and 0.10 (±0.03) pptv respectively. The trajectory model results are consistent with this effect, predicting HO_x values slightly lower than observed. If we compare these mixing ratios with a model calculation in which we do not include reaction (3), predicted OH and HO_2 levels would be more than a factor of 10 higher. Not including either (2) or (3) results in modeled HO_x being 5 times higher than observations. Note that CH_3OO is measured with 50% efficiency in the HO_2 channel, and that this could introduce a bias in the HO_2 observations by up to 15% inside the vortex.

The steady state assumption for HOCl* (reaction (6)) no longer holds for temperatures below 195 K. In these regions, rates for heterogeneous and gas phase loss become similar, and our time-dependent model calculations yield HOCl values 50% lower than steady state calculations would predict. We have therefore included a correction factor for the HOCl* values derived from measured ClO and HO_2 poleward of 66°S (panel e in Plate 2 b).

Direct heterogeneous loss of OH itself on sulfate aerosols via $OH + HNO_3 \rightarrow H_2O + NO_3$ is too slow to compete with the similar homogeneous reaction [*Danilin et al.*, 1994a], and the heterogeneous loss of HO_2 on sulfate aerosol via reaction $HO_2 + HO_2 \rightarrow H_2O_2$ is very minor in importance compared with other gas phase reactions [*Danilin et al.*, 1994a].

A more thorough discussion of the relative importance of (2) and (3) on the HO_x budget in the polar environment is presented by K96 in the context of the July 30, 1994, ASHOE/MAESA ER-2 flight.

6.3. Role of Aerosol Surface Type

In all of the above we have assumed that aerosols were present in the form of supercooled ternary solutions $H_2SO_4/HNO_3/H_2O$ which grow in volume as HNO_3 and H_2O condense at temperatures below ~193 K (Figure 6). Observations of total nitrogen for this flight indeed show the presence of HNO_3 in the aerosol phase [*Del Negro et al.*, this issue]. In situ observations of the particle composition and phase suggest a rather more composite picture during this flight. In particular, aerosol samples collected at 67°S inside a PSC show the presence of type I and type II particles with an effective radius of 7 μm [*Goodman et al.*, 1997]. These crystals most likely originated from higher altitudes and were falling through the air sampled by the ER-2. Because of their low observed concentrations, the contribution of types I and II PSCs to the total surface area is small (less than 5%, *Goodman et al.*, [1997]).

Our calculations show an additional increase in chlorine activation of less than 2% if we include, in addition to supercooled aerosols, both types I and II aerosols (at a surface area of 0.2 $\mu m^2/cm^3$ for the last 12 hours of the trajectory, corresponding to the observations by Goodman et al.). This particular model calculation is illustrated by the plus symbol in Plate 2 a (case 3). Furthermore, wire impactor measurements during this flight show that up to 30% of the sulfate aerosols were frozen at 64°S on the northbound leg of the flight [*Goodman et al.*, 1997]. If we assume that frozen sulfate aerosols were present with a surface area of 0.8 $\mu m^2\ cm^{-3}$, in addition to background aerosols, we obtain 0.03 ppbv more ClO (star symbol in Plate 2 a, case 4).

Thus for the ER-2 flight of July 28 the high ClO levels seem to have been mainly caused by heterogeneous reaction (1) on supercooled sulfate aerosols surfaces. These results are in agreement with independent studies by *Kawa et al.* [1997], *Dye et al.* [1996] and *Del Negro et al.* [this issue] for the same ASHOE/MAESA flight. Because of their low concentrations, types I and II PSCs did not contribute much to chlorine activation. When present, frozen aerosols have the potential of increasing chlorine activation, but under the conditions studied here, their role was comparable to sulfate aerosols.

6.4. Dependence on Temperature History

For the last 12 hours before ER-2 observations the temperature histories derived from the NMC analysis [*Kawa et al.*, 1997] compare well with the ECMWF trajectories used in this study: the onset of the rapid cooling is very similar in the two analyses. The slightly colder temperatures (by up to 2 K) from NMC result in chlorine activation which is 10% higher than shown in Plate 2 a. Between days 200 and 208 (see Figure 7 a), the NMC analysis yields temperatures 2-3 K colder than ECMWF, but as temperatures are generally above 200 K, very little chlorine activation takes place and this does not affect our results.

7. Recent Heterogeneous Processing: August 6

Observations during the flight of August 6, 1994, are summarized in Plate 3 a and 3 b. The temperatures measured aboard the ER-2 were, on the average, 10 K warmer than on July

28, 1994. The lowest temperatures reached were close to 200 K (top of Plate 3 b). Ten-day back trajectories show that southward of 64°S this air was repeatedly exposed to temperatures well below NAT formation temperatures (Figure 7 b) and had been warming on the last few days before being sampled by the instruments aboard the ER-2. HCl levels outside the vortex (equatorward of 64°S, as defined by the polar jet maximum) are generally higher than for July 28 because the air sampled contained more Cl_y, as indicated by the lower N_2O values measured.

7.1. Model Results Along Trajectories

As in section 6.1, we first assume that the aerosols are in the liquid phase and that they incorporate HNO_3 to form STS at low temperatures. Model calculations along trajectories are compared to the observations in Plate 3 . The latitudinal extent of enhanced ClO and Cl_2O_2 is well reproduced by the model. If we assume no previous processing event, modeled HCl levels poleward of 65°S are much too high: over the 10 days of the calculation, most of $ClONO_2$ has been consumed, and HCl lacks a partner to be further depleted. In a fashion similar to that described for the previous flight, we initialize the chlorine reservoirs assuming that 30% of Cl_y has been processed and repartitioned into $ClONO_2$ (case 2, triangles), as suggested by observations on July 28, 1994.

In this case, model results for HCl are in better agreement with the observations south of 64°S. The total depletion of HCl, however, generates levels of OH and HO_2 inside the vortex that are too high by a factor of 2 compared to observations (Plate 3 b). Furthermore, model calculations for OH predict a local maximum inside the vortex, while observations show a minimum. This reflects the accumulation of HOCl in the model which can no longer react with HCl via (3) and as a consequence acts as a source of HO_x.

On the other hand, if we assume formation of NAT PSCs (case 3, pluses), our model calculations are in better agreement with the observations of HO_x at the inner vortex edge. Indeed, as the temperature was oscillating well below 195 K for air parcels inside the vortex 10 days prior to the intercept, we might expect the phase of the aerosols to be NAT, water ice, and/or frozen particles, depending on the temperature thresholds reached. We next examine the sensitivity of our model calculations to the assumed aerosol composition, which has an impact on both the surface reactivities and the growth properties of the particles.

7.2. Model Sensitivity to Aerosol Composition

For the August 6, 1994, flight, no continuous aerosol measurements are available. However, the samples collected by the Ames wire impactor experiment [*Pueschel et al.*, 1989] show a relatively low amount of background aerosols (~1 $\mu m^2\ cm^{-3}$), all in the liquid phase. This is consistent with volume observations obtained a few days later on August 8 and 10, 1994, with the continuous aerosol measurements, which are a factor of 2 lower than on July 28 and 30, 1994 (~2-3 $\mu m^2\ cm^{-3}$ outside of the PSC). One possible explanation for this phenomenon could be the growth and subsequent sedimentation of large aerosols (>1

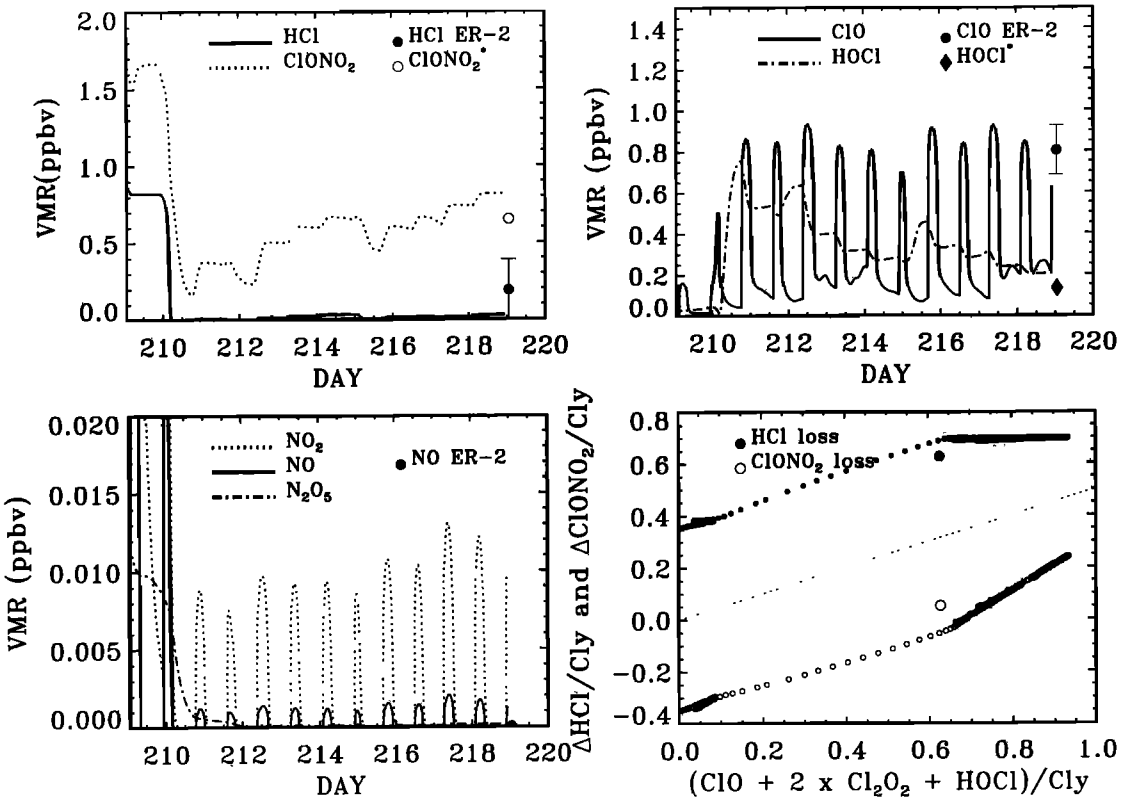

Figure 9. Inside the vortex: evolution of model calculations along a trajectory starting on July 26 (day 209) and ending on August 6, 1994 (67.2°S, 172.5°E, at 22:45 UT). Parcel 12 in Plate 3 a. Temperature history in Figure 7. The initialization assumes pre processing of the reservoirs. We assume formation of STS on background sulfate aerosols. In order to conserve the stoichiometry, $\Delta HCl/Cl_y$ and $\Delta ClONO_2/Cl_y$ are plotted as a function of $(ClO + 2\ Cl_2O_2 + HOCl)/Cl_y$.

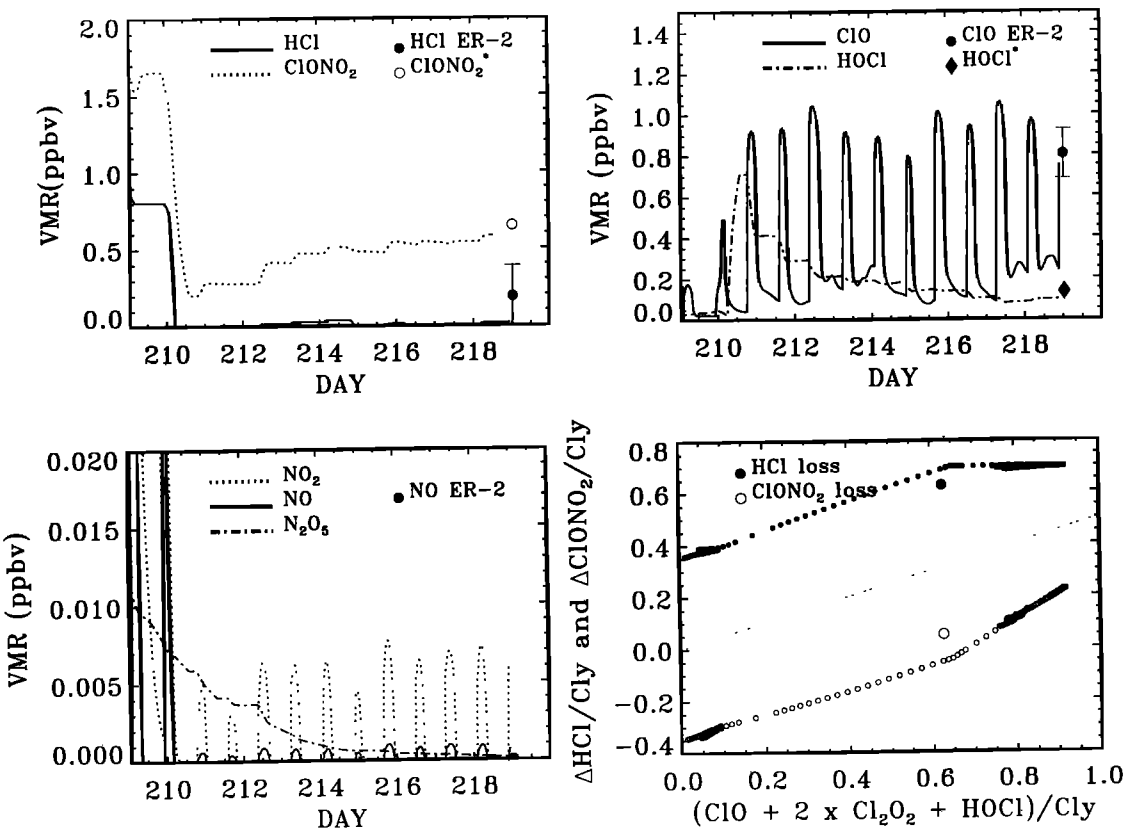

Figure 10. Inside the vortex: same as Figure 9, assuming NAT (when $T_{ICE}<T<T_{NAT}$) and ice (when $T<T_{ICE}$) PSC formation.

μm) when cold temperatures are repeatedly reached during the 8-10 day period separating the flights.

The stratospheric temperature at which NAT particles are formed is not well known and seems to depend on the state of background particles [*Rosen et al.*, 1993] as well as on the amount of condensing vapors [*Hanson and Mauersberger*, 1988]. Observations imply a barrier to the thermodynamic formation of NAT, which tends to form 3 K below T_{NAT} [*Fahey et al.*, 1989]. It is possible that surfaces need some 'accommodation' before NAT readily forms [*Zhang et al.*, 1996]. Or, in a more complex manner, cooling and warming cycles could cause selective formation of different surface types [*Tabazadeh and Toon*, 1995].

We can construct the following scenario. During the first cooling cycle NAT forms on background liquid aerosols at 3 K supersaturation (T_{NAT} - 3K). Once $T>T_{NAT}$, NAT evaporates and leaves behind liquid aerosols and SAT. The next formation cycle may take place at 0 K supersaturation, due to preactivation of the background surfaces [*Zhang et al.*, 1995]. When temperatures decrease below the ice formation temperature (for parcels 13 to 15, as numbered on Plate 3 a), we assume formation of type II PSCs with a radius of 10 μm. In these calculations we do not include the effects of aerosol sedimentation out of the considered air parcel or originating from air masses above. This phenomenon was observed in the redistribution of H_2O and NO_y observations during the ER-2 dive (~16 km) during this flight [*Tuck et al.*, 1995], but not elsewhere [*Keim et al.*, this issue].

In Figures 9 and 10 we compare the different behavior of reactive species for the STS case and for the described PSC scenario, with sulfate aerosols acting as the background surfaces. These Lagrangian calculations correspond to the temperature history shown in Figure 7 b (parcel 12), and they assume previous processing of HCl as discussed above. For the STS case in Figure 9, $ClONO_2$ and HCl are rapidly lost via reaction (1). Once all the HCl has been consumed on day 210, the heterogeneous processing of $ClONO_2$ continues through (2) and generates very high levels of HOCl (~0.75 ppbv). As illustrated in Figure 5, the hydrolysis of $ClONO_2$ on sulfate aerosols proceeds more rapidly if there is no competition from its reaction with HCl. Small excursions of the air parcel to lower latitudes (up to 58°S) allow $ClONO_2$ to reform by reaction of ClO with NO_2 resulting from the photochemical conversion of HNO_3 (at times 212.5 and 216). Repeated exposures to cold temperatures continue the processing of $ClONO_2$ via (2) and maintain high ClO and HOCl levels. Note the strong diurnal variation of ClO which is due to the photolysis of Cl_2O_2 during the day. At night the ClO dimer is the dominant Cl_x species. For the PSC scenario in Figure 10, further depletion of $ClONO_2$ after day 210 takes place through hydrolysis of $ClONO_2$ on ice (which forms in the model on day 210.25 for 12 hours, when temperatures decrease below T_{ice} = 189 K). Hydrolysis of $ClONO_2$ on NAT surfaces is much slower than on ice or sulfate aerosols; therefore, the high levels of HOCl first produced on day 210 cannot be maintained through (2) on NAT and slowly decrease via photolysis, and heterogeneous reaction with both HCl and HBr. After 2-3 days, HOCl levels are controlled by pure gas phase chemistry. As a consequence of these lower HOCl mixing ratios, the resulting OH and HO_2 are in better agreement with observations for the PSC case (case 3 in Plate 3 b) rather than for the STS case (case 2). We have tested the sensitivity of our results on the occurrence of ice PSCs on day 210 (8 days prior to the ER-2 flight) and found

that the formation of ice and assumptions on surface area have very little impact (± 10%) on the HO_x levels at the end of the trajectory, due to the rapid relaxation time of HOCl.

Note that both model cases predict very low HCl (0.05 ppbv), while the observations seem to suggest a higher value (0.17 ± 0.2 ppbv) At these mixing ratios the signal-to-noise ratio is poor as reflected by the large error bars, and it is difficult to determine how much HCl is present.

We have used a sticking coefficient of 0.001 for (2) on NAT as recommended by DeMore *et al.* [1994]. However, laboratory results range between 10^{-6} and 0.02 [*Leu et al.*, 1991; *Moore et al.*, 1990]. If we use a value of 0.01, our calculations yield slightly larger HOCl levels and further improvement in the agreement with the HO_x observations.

Thus, compared to the July 28 flight, during August 6, relatively high levels of OH and HO_2 were measured inside the vortex: 0.1 (± 0.03) and 0.5 (± 0.15) pptv, respectively, as opposed to 0.025 and 0.1 pptv on July 28 for similar solar zenith angles. This source of HO_x is supplied by high HOCl mixing ratios on August 6 (Plate 3 b). In this case, the sustained near-zero HCl mixing ratios contribute to turning off the main sink for HOCl, reaction (3). Comparison between model calculations and observations support the laboratory measured small reactivity of (2) on NAT surfaces, as opposed to the faster rates for the same reaction on sulfate aerosols and type II PSCs.

The bottom right-hand panels of Figure 9 and 10 show the two types of slopes obtained for ΔHCl and $\Delta ClONO_2$ which were discussed in section 4 for case 4.4. : as reaction (1) proceeds, the 1:2 slope develops, but when all the HCl is depleted, $ClONO_2$ continues to produce active chlorine through (2) on sulfate aerosols or type II PSCs, forming the 1:1 slope. The different PSC composition assumed for these two cases do not have a large effect on active chlorine and HCl levels, and therefore there is not much difference in the patterns on these two bottom plots.

The wire impactor measurements on July 28, 1994, have clearly shown that SAT could be present in the polar environment Thus we have conducted a test case where we have assumed the background aerosols to be all frozen (at a surface area of 1 $\mu m^2\ cm^{-3}$), once ice formation temperature is reached and that NAT subsequently forms on these surfaces. The results obtained are very similar to those shown in Figure 10, due to heterogeneous reactivities for SAT which are comparable to those on sulfate aerosols.

From our photochemical analysis of the ER-2 observations, we deduce that the amount of chlorine activation is fairly independent of the composition of PSCs (STS, NAT, ice), due to the very similar reactivity of (1) on all these surfaces (Figure 5). However,the composition of PSCs can have a large impact on the amount the denitrification in the vortex [*Del Negro et al.*, this issue]. Thus on the basis of ClO and HCl observations alone, no differentiation is possible. On the other hand, reaction (2) has very different rates for these surfaces, and its impact on HO_x levels has been used to deduce the possible formation of type I PSCs in air sampled on August 6, 1994. In this manner, OH and HO_2 can be very sensitive indicators of the degree of processing of HCl and may exhibit different signatures depending on the type of heterogeneous surfaces that affected chlorine activation.

7.3. Dependence on Temperature History

The temperature histories obtained with the isentropic NMC fields tend to be 3 K colder than the ECMWF trajectories close to the edge of the vortex (62°-66°S) for August 6, 1994. The temperatures begin to diverge after one day along the back trajectory. This difference has a large impact on the photochemical calculations: the colder NMC temperatures lead to 2-5 times more chlorine activation near the edge of the vortex (the latitudinal gradient in model-calculated ClO is displaced in latitude by 1 5° north compared to ER-2 observations). Outside of the vortex (south of 62°S) and deeper inside the vortex (north of 66°S), the analyses are similar and yield very similar results for HCl, ClO, HO_x and NO. The observed difference could be due in part to the strong cooling rate at the edge of the vortex which is taken into account in the ECMWF three-dimensional trajectories but not in the GSFC isentropic trajectories. Future comparisons between observed and derived cooling rates would be required to resolve those differences.

7.4. Implications for Ozone Loss

In response to the chlorine activation, ozone begins to decrease in June continuing until the springtime when higher sun levels fuel the chemical cycles involving halogens [*Molina and Molina*, 1987; *McElroy et al.*, 1986]. In situ O_3 observations during ASHOE/MAESA show that 25% of O_3 has been depleted by early August [*Tuck et al.*, 1995].

Figure 10 shows that active chlorine levels had been elevated for at least 1 week prior to the ER-2 flight on August 6, 1994. From our photochemical back trajectory calculations for this 10 day period, we obtain an average ozone loss of 30 ppbv day^{-1}. If this rate of loss can be maintained, then by mid-October, very little ozone is left. Indeed, air with extremely depleted O_3 levels (99% loss) was sampled by the ER-2 on two occasions on October 10 and 13 (W96b). However, more generally ER-2 observations at this time show ozone losses in excess of 75% at the highest latitudes. These different amounts of ozone loss observed in the edge region of the vortex probably reflect varying degrees of mixing and exposure to sunlight which result in separate regimes of chlorine recovery (W96b).

8. Summary and Conclusions

Measurements of HCl and ClO during the Antarctic winter of 1994 indicate chemical processing of the chlorine reservoir HCl to active chlorine via the heterogeneous reaction $HCl + ClONO_2 \rightarrow Cl_2 + HNO_3$. This processing is diagnosed by large losses in HCl, increases in ClO, and a slope of 1:2 for ΔHCl versus ClO + 2 Cl_2O_2 , consistent with the stoichiometry of the above reaction. The high amounts of $ClONO_2$ inferred in this study (and forming the $ClONO_2$ "collar") are generated by PSC processing followed by excursions into sunlight. While chlorine activation begins with 60-75% of Cl_y as HCl, the near-total removal of HCl can take place from excursions in and out of sunlight, with resupply of $ClONO_2$ and HOCl which provide oxidation partners for HCl.

Examination of two separate ER-2 flights with a box model along trajectories has confirmed the dominant role of reaction (1) in generating the observed HCl loss and ClO production. Evidence of the reaction HCl + HOCl on sulfate aerosols was found by its impact on HO_x levels. On the basis of high HO_x observations under very low HCl conditions, we deduce the likely formation of type I PSCs identified by their slow rate for $ClONO_2 + H_2O \rightarrow HOCl + H_2O$. Furthermore, in this environment, the exact physical and chemical state of the surfaces providing sites for heterogeneous reactions does not significantly change the amount of chlorine activation generated.

Together, these findings quantitatively confirm the central role of heterogeneous chemistry on sulfate aerosols and PSCs in the Antarctic stratosphere and point to the importance of

latitudinal excursions in the edge region of the vortex. The consistency between model calculations and observations strengthens our confidence in the current understanding of stratospheric gas phase and heterogeneous polar chemistry controlling chlorine activation.

Acknowledgments. The authors would like to thank H Nair for providing the original modifications to the photochemical Lagrangian code K Carslaw made available his code for ternary solution growth We thank D Fahey for the ASHOE/MAESA NO and NO_y data, E. Keim and L Del Negro for valuable discussions, and L. Mickley for helpful comments. The authors also thank two reviewers for their comments. Additional field operations support of ALIAS was provided by M.Tuchscherer and G. Flesch Part of the research described in this paper was carried out by the Jet Propulsion Laboratory, California Institute of Technology, under contract with the National Aeronautics and Space Administration (NASA). This research is also supported in part by NASA grant NAGW-413 to the California Institute of Technology

References

Abbatt, J P D., Heterogeneous reaction of HOBr and HCl on ice surfaces at 228 K, *Geophys. Res. Lett* , *21*, 665-668, 1994

Abbatt, J P D , Heterogeneous reactions of BrO and ClO – Evidence for BrO surface recombination and reaction with HNO_3/SO_4^{2-}, *Geophys Res Lett* , *21*, 665-668, 1996.

Abbatt, J. P. D , and M. J. Molina, The heterogeneous reaction of HOCl + HCl → Cl_2 + H_2O on ice and nitric acid trihydrate· Reaction probabilities and stratospheric implications, *Geophys. Res. Lett* , *19*, 461-464, 1992.

Anderson, J. G., D. W. Toohey, and W H. Brune, Free radicals within the Antarctic vortex· The role of CFCs in Antarctic ozone loss, *Science*, *251*, 39-46, 1991.

Austin, J , et al , Lagrangian photochemical modeling studies of the 1987 Antarctic spring vortex, 2. Seasonal trends in ozone, *J. Geophys Res* , *94*, 16,717-16,735, 1989.

Baumgardner, D., J. E. Dye, B. W. Gandrud, and R. G Knollenberg, Interpretation of measurements made by the forward scattering spectrometer probe (FSSP-300) during the Airborne Arctic Stratospheric Expedition, *J. Geophys Res* , *97*, 8035-8046, 1992.

Brune, W H., J G Anderson, and K. R. Chan, In situ observations of ClO in the Antarctic: ER-2 aircraft results from 54°S to 72°S latitude, *J Geophys. Res.*, *94*, 16,649-16,663, 1989.

Burkholder, B , Ultraviolet-absorption cross-sections of Cl_2O_2 between 210 and 410 nm, *J. Phys. Chem* , *94*, 687-695, 1990.

Carslaw, K. S , B P. Luo, S. L Clegg, T Peter, P. Brimblecombe, and P.J Crutzen, Stratospheric aerosol growth and HNO_3 gas phase depletion from coupled HNO_3 and water uptake by liquid particles, *Geophys Res. Lett.*, *21*, 2479-2482, 1994.

Carslaw, K S., B P. Luo, and T Peter, An analytic expression for the composition of aqueous HNO_3-H_2SO_4 stratospheric aerosols including gas phase removal of HNO_3, *Geophys. Res. Lett.*, *22*, 1877-1880, 1995.

Chan, A. Y., *et al.*, A comparison of measurements from ATMOS and instruments aboard the ER-2 aircraft – Tracers of atmospheric transport, *Geophys. Res. Lett.*, *23*, 2389-2392, 1996.

Chipperfield, M P , J. A. Pyle, C. E. Blom, N. Glatthor, M. Hopfner, T. Gulde, C. Piesch, and P. Simon, The variability of $ClONO_2$ and HNO_3 in the Arctic polar vortex: Comparison of Transall Michelsen interferometer for passive atmospheric sounding measurements and three-dimensional model results, *J Geophys Res, 100*, 9115-9129, 1995

Crutzen, P. J., and F. Arnold, Nitric acid cloud formation in the cold Antarctic stratosphere: A major cause for the springtime "ozone hole", *Nature*, *324*, 651-655, 1986.

Crutzen, P J., R. Müller, C Brühl, and T Peter, On the potential importance of the gas phase reaction CH_3O_2 + ClO → ClOO + CH_3O and the heterogeneous reaction HOCl + HCl → H_2O + Cl_2 in "ozone hole" chemistry, *Geophys. Res. Lett.*, *19*, 1113-1116, 1992.

Danilin, M. Y., and J. C. McConnell, Heterogeneous reactions in a stratospheric box model· a sensitivity study, *J. Geophys. Res.*, *99*, 25,681-25,696, 1995a.

Danilin, M Y. and J. C. McConnell, Stratospheric effects of bromine activation on sulfate aerosols, *J. Geophys. Res.*, *100*, 11,237-11,243, 1995b.

Del Negro, L. A., *et al.*, Evaluating the role of NAT, NAD, and liquid $H_2SO_4/H_2O/HNO_3$ solution in Antarctic polar stratospheric cloud aerosol· observations and implications, *J. Geophys. Res.*, this issue.

DeMore, W. B., S. P. Sander, D. M. Golden, R F. Hampson, M. J. Kurylo, C J. Howard, A. R. Ravishankara, C. E. Kolb, and M J Molina, Chemical kinetics and photochemical data for use in stratospheric modeling, in *Evaluation 10*, *JPL Pub 94-26*, Jet Propul Lab., Pasadena, Calif., 1994.

Dye, J. E., *et al.*, In situ observations of an Antarctic polar stratospheric cloud – Similarities with Artic observations, *Geophys Res Lett* , *23*, 1913-1916, 1996.

Elkins, J. W., et al., Airborne gas chromatograph for the in situ measurements of long-lived species in the upper troposphere and lower stratosphere, *Geophys Res. Lett.*, *23*, 347-350, 1996

Fahey, D W., K. K. Kelly, S. R Kawa, A. F. Tuck, M. Loewenstein, K R Chan, and L E Heidt, Observations of denitrification and dehydration in the winter polar stratospheres, *Nature*, *344*, 321-324, 1990

Fahey, D W., K. K. Kelly, G V. Ferry, L R. Poole, J. C. Wilson, D. M Murphy, M. Loewenstein, and K R Chan, *In situ* measurements of reactive nitrogen, total water, and aerosol in a polar stratospheric cloud in the Antarctic, *J Geophys. Res.*, *94*, 11,299-11,315, 1989

Fahey, D W , et al , In situ measurements constraining the role of sulfate aerosols in mid-latitude ozone depletion, *Nature*, *363*, 509-514, 1993.

Farman, J C , G C Gardiner, and J. D. Shanklin, Large losses of total ozone in Antarctica reveal seasonal ClO_x/NO_x interaction, *Nature*, *315*, 207-210, 1985.

Farmer, C B , G. C. Toon, P. W. Schaper, J - F. Blavier, and L. L. Lowes, Stratospheric trace gases in the spring 1986 Antarctic atmosphere, *Nature*, *329*, 126-130, 1987.

Gao, R S , et al , Partitioning of reactive nitrogen reservoir in the lower stratosphere of the southern hemisphere: Observations and modeling, *J Geophys Res.*, *102*, 3934-3943, 1997.

Goodman, J., S. Verma, R F. Pueschel, P. Hamill, G. V. Ferry, and D. Webster, New evidence for size and composition of polar stratospheric cloud particles, *Geophys. Res. Lett* , *24*, 615-618, 1997.

Hanson, D. R., and K. Mauersberger, Laboratory studies of the nitric acid trihydrate· Implications for the south polar stratosphere, *Geophys Res Lett.*, *15*, 855-858, 1988.

Hanson, D. R., and A. R Ravishankara, Reaction of $ClONO_2$ with HCl on NAT, NAD, frozen sulfuric acid, and hydrolysis of N_2O_5 and $ClONO_2$ on frozen sulfuric acid, *J Geophys. Res* , *98*, 22,931-22,936, 1993

Hanson, D. R., and A R. Ravishankara, Heterogeneous chemistry of bromine species in sulfuric-acid under stratospheric conditions, *Geophys Res Lett.*, *22*, 385-388, 1995.

Hanson, D R , and A R. Ravishankara, Reactive uptake of $ClONO_2$ onto sulfuric-acid due to reaction with HCl and H_2O, *J Phys. Chem.*, *98*, 5728-5735, 1994

Hanson, D. R., A R. Ravishankara, and S. Solomon, Heterogeneous reactions in sulfuric acid aerosols. a framework for model calculations, *J Geophys. Res.*, *99*, 3615-3630, 1994.

Hofmann, D. J., S. J. Oltmans, J. A. Lathrop, J. M. Harris, and H. Vömel, Record low ozone at the South Pole in the spring of 1993, *Geophys. Res Lett.*, *21*, 421-424, 1994.

Huder, K. J., and W B DeMore, Absorption cross sections of the ClO dimer, *J. Phys Chem.*, *99*, 3905-3908, 1995.

Jaeglé, L., Stratospheric chlorine and nitrogen chemistry· Observations and modeling, Ph D thesis, Calif. Insti. of Technol., Pasadena, 1996.

Jaeglé, L., Y L. Yung, G. C. Toon, B. Sen, and J.- F. Blavier, Balloon observations of organic and inorganic chlorine in the stratosphere· The role of $HClO_4$ production on sulfate aerosols, *Geophys. Res. Lett.*, *23*, 1749-1752, 1996

Jones, R L., et al., Lagrangian photochemical modeling studies of the 1987 Antarctic spring vortex, 1, Comparison with AAOE observations, *J. Geophys. Res.*, *94*, 11,529-11,558, 1989.

Jonsson, H H., et al., Performance of a focused cavity aerosol spectrometer for measurements in the stratosphere of particle size in the 0.06-2.0 μm - diameter range, *J. Atmos. Ocean. Technol.*, *12*, 115-129, 1995.

Kawa, S. R., D W. Fahey, L. E. Heidt, W. H. Pollock, S. Solomon, D. E. Anderson, M Loewenstein, M. H. Proffitt, J. J. Margitan, and K R Chan, Photochemical partitioning of the reactive nitrogen and chlorine reservoirs in the high-latitude stratosphere, *J. Geophys. Res.*, *97*, 7905-7923, 1992.

Kawa, S R., et al , Activation of chlorine in sulfate aerosol as inferred from aircraft observations, *J. Geophys. Res.*, *102*, 3921-3933, 1997.

Keim, E. R., et al., Measurements of the NO_y-N_2O correlation in the lower stratosphere: Latitudinal and seasonal changes and model comparisons, *J. Geophys. Res.*, this issue.

Kelly, K. K., et al., Dehydration in the lower Antarctic stratosphere during late winter and early spring 1987, *J. Geophys. Res.*, *94*, 11,317-11357, 1989.

Kenner, R. D., I. C. Plumb, and K. R. Ryan, Laboratory measurements of the loss of ClO on pyrex, ice and NAT at 183 K, *Geophys. Res. Lett.*, *20*, 193-196, 1993.

Lary, D. J, M. P. Chipperfield, R. Toumi, and T. Lenton, Atmospheric heterogeneous bromine chemistry, *J. Geophys. Res.*, *101*, 1489-1504, 1996

Lefèvre, F., G. P. Brasseur, I. Folkins, A. K. Smith, and P. Simon, Chemistry of the 1991-1992 stratospheric winter – Three-dimensional model simulations, *J. Geophys. Res.*, *99*, 8183-8195, 1994

Leu, M. T., Laboratory studies of sticking coefficients and heterogeneous reactions important in the Antarctic stratosphere, *Geophys. Res. Lett.*, *15*, 17-20, 1988

Leu, M. T., S. B. Moore, and L. F. Keyser, Heterogeneous reactions of chlorine nitrate and hydrogen chloride on type I polar stratospheric clouds, *J. Phys. Chem.*, *95*, 7763-7771, 1991.

Liu, X., R. D. Blatherwick, F. J. Murcay, J. G. Keys, and S. Solomon, Measurements and model calculations of HCl column amounts and related parameters over McMurdo during the austral spring in 1989, *J. Geophys. Res.*, *97*, 29,795-29804, 1992.

Lutman, E. R., J. A. Pyle, R. L. Jones, D. J. Lary, A. R. McKenzie, I. Kilbane-Dawe, N. Larsen, and B. Knudsen, Trajectory model studies of Cl_x activation during the 1991/92 northern hemispheric winter, *Geophys. Res. Lett.*, *21*, 1419-1422, 1994a.

Lutman, E. R., R. Toumi, R. L. Jones, D. J. Lary, and J. A. Pyle, Box model studies of Cl_x deactivation and ozone loss during the 1991/92 northern hemispheric winter, *Geophys. Res. Lett.*, *21*, 1415-1418, 1994b

Manney, G. L., and R. W. Zurek, Interhemispheric comparison of the development of the stratospheric polar vortex during fall. A three-dimensional perspective for 1991-1992, *Geophys. Res. Lett.*, *20*, 1275-1278, 1993

Marti, J., and K. Mauersberger, A survey and new measurements of ice vapor pressure at temperatures between 170 and 250 K, *Geophys. Res. Lett.*, *20*, 363-366, 1993

McCormick, M. P., H. M. Steele, P. Hamill, W. P. Chu, and T. J. Swissler, Polar stratospheric cloud sightings by SAM II, *J. Atmos. Sci.*, *39*, 1387-1397, 1982.

McElroy, M. B., R. J. Salawitch, S. C. Wofsy, and J. A. Logan, Reductions of antarctic ozone due to synergestic interactions of chlorine and bromine, *Nature*, *321*,759-762, 1986.

Molina, L. T., and M. J. Molina, Production of Cl_2O_2 from the self-reaction of the ClO radical, *J. Phys. Chem.*, *91*, 433-436, 1987

Molina, M. J., and F. S. Rowland, Stratospheric sink for chlorofluoromethanes. Chlorine atom catalyzed destruction of ozone, *Nature*, *249*, 810-814, 1974.

Molina, M. J., R. Zhang, P. J. Wooldridge, J. R. McMahon, J. E. Kim, H. Y. Chang, and K. Beyer, Physical chemistry of the $H_2SO_4/HNO_3/H_2O$ system: implications for the formation of polar stratospheric clouds and heterogeneous chemistry, *Science*, *216*, 1418-1423, 1993.

Moore, S. B., L. F. Keyser, M. T. Leu, R. P. Turco, and R. H. Smith, Heterogeneous reactions on nitric acic trihydrate, *Nature*, *345*, 333-335, 1990.

Müller R., and P. J. Crutzen, A possible role of galactic cosmic-rays in chlorine activation during polar night, *J. Geophys. Res.*, *98*, 20,483-20,490, 1993.

Nair, H., Photochemical processes in the atmospheres of Earth and Mars, Ph.D. Thesis, Calif. Inst. of Technol., Pasadena, 1996

Oelhaf, H., T. von Clarmann, H. Fischer, F. Friedlvallon, C. Fritzsche, A. Linden, C. Piesch, M. Seefeldner, and W. Volker, Stratospheric $ClONO_2$, HNO_3 and O_3 profiles inside the Arctic vortex from MIPAS-B limb emission spectra obtained during EASOE, *Geophys. Res. Lett.*, *21*, 1263-1266, 1994.

Plumb, R. A., and M. K. Ko, Interrelationships between mixing ratios of long-lived stratopsheric constituents, *J. Geophys. Res.*, *97*, 10,145-10,156, 1992.

Prather, M. J., More rapid ozone depletion through the reaction of HOCl with HCl on polar stratospheric clouds, *Nature*, *355*, 534-537, 1992.

Proffitt, M.H., et al., In situ ozone measurements within the 1987 Antarctic ozone hole from a high-altitude ER-2 aircraft, *J. Geophys. Res.*, *94*, 16,547-16,556, 1989

Pueschel, R. F., et al., Condensed nitrate, sulfate, and chloride in Antarctic stratospheric aerosols, *J. Geophys. Res.*, *94*, 11,271-11,284, 1989

Pyle, J. A., et al., An overview of the EASOE campaign, *Geophys. Res. Lett.*, *21*, 1191-1194, 1994.

Rattigan, O.V., D. J. Lary, R. L. Jones, and R. A. Cox, UV-visible absorption cross sections of gaseous Br_2O and HOBr, *J. Geophys. Res.*, *101*, 23021-23033, 1996

Roche, A. E., J. B. Kumer, and J. L. Mergenthaler, CLAES observations of $ClONO_2$ and HNO_3 in the Antarctic stratosphere, between June 15 and September 17, 1992, *Geophys. Res. Lett.*, *20*, 1223-1226, 1993

Roche, A. E., J. B. Kumer, J. L. Mergenthaler, R. W. Nightingale, W. G. Uplinger, G. A. Ely, J. F. Potter, D. J. Wuebbles, P. S. Connell, and D. E. Kinnison, Observations of lower-stratospheric $ClONO_2$, HNO_3, and aerosol by the UARS CLAES experiment between January 1992 and April 1993, *J. Atmos. Sci.*, *51*, 2877-2902, 1994.

Rosen, J. M., N. T. Kjome, and S. J. Oltmans, Simultaneous ozone and polar stratopsheric cloud observations at South Pole Station during winter and spring 1991, *J. Geophys. Res.*, *98*, 12,741-12,751, 1993

Russell, J. M., III, *et al.*, The Halogen Occultation Experiment, *J. Geophys. Res.*, *98*, 10,777-10,797, 1993.

Salawitch, R. J., et al., Chemical loss of ozone in the Arctic polar vortex in the winter of 1991-1992, *Science*, *261*, 1146-1149, 1993.

Salawitch, R. J., S. C. Wofsy, and M. B. McElroy, Influence of polar stratospheric clouds on the depletion of Antarctic ozone, *Geophys. Res. Lett.*, *15*, 871-874, 1988.

Salawitch, R. J., et al., Implications for the heterogeneous production of HNO_3, *Geophys. Res. Lett.*, *21*, 2551-2554, 1994.

Sander, S. P., R. R. Friedl, and Y. L. Yung, Rate of formation of the ClO dimer in the polar stratosphere: Implications for ozone loss, *Science*, *245*, 1095-1098, 1989.

Santee, M. L., W. G. Read, J. W. Waters, L. Froidevaux, G. L. Manney, D. A. Flower, R. F. Jarnot, R. S. Harwood, and G. E. Peckham, Interhemispheric differences in polar stratospheric HNO_3, H_2O, ClO, and O_3 from UARS MLS, *Science*, *267*, 849-852, 1994.

Schauffler, S. M., L. E. Heidt, W. H. Pollock, T. M. Gilpin, J. F. Vedder, S. Solomon, R. A. Lueb, and E. L. Atlas, Measurements of halogenated organic-compounds near the tropical tropopause, *Geophys. Res. Lett.*, *20*, 2567-2570, 1993

Schoeberl, M. R., and D. L. Hatmann, The dynamics of the stratospheric polar vortex and its relation to springtime ozone depletion, *Science*, *251*, 46-52, 1991

Schoeberl, M. R., L. R. Lait, P. A. Newman, and J. E. Rosenfeld, The structure of the polar vortex, *J. Geophys. Res.*, *97*, 7859-7882, 1992.

Schoeberl, M. R., et al., The evolution of ClO and NO along air parcel trajectories, *Geophys. Res. Lett.*, *20*, 2511-2514, 1993.

Schoeberl, M. R., M. L. Luo, and J. E. Rosenfield, An analysis of the Antarctic HALOE trace gas observations, *J. Geophys. Res.*, *100*, 5159-5172, 1995.

Scott, S. G., T. P. Bui, K. R. Chan, and S. W. Bowen, The meteorological measurement system on the NASA ER-2 aircraft, *J. Atmos. Oceanic Technol.*, *7*, 525-540, 1990.

Solomon, S., Progress towards a quantitative understanding of antarctic ozone depletion, *Nature*, *347*, 347-354, 1990.

Solomon, S., R. R. Garcia, F. S. Rowland, and D. J. Wuebbles, On the depletion of antarctic ozone, *Nature*, *321*, 755-758, 1986.

Solomon, S., R. W. Sanders, R. R. Garcia, and J. G. Keys, Increased chlorine dioxide over Antarctica caused by volcanic aerosols from Mt. Pinatubo, *Nature*, *363*, 245-248, 1993

Steele, H. M., P. Hamill, M. P. McCormick, and T. J. Swissler, The formation of polar stratospheric clouds, *J. Atmos. Sci.*, *40*, 2055-2067, 1983.

Tabazadeh, A., and O. B. Toon, Freezing behavior of stratospheric sulfate aerosols inferred from trajectory studies, *Geophys. Res. Lett.*, *22*, 1725-1728, 1995.

Tabazadeh, A., R. P. Turco, and M. Z. Jacobson, A model for studying the composition and chemical effects of stratospheric aerosols, *J. Geophys. Res.*, *99*, 12,897-12,914, 1994.

Tolbert, M. A., M. J. Rossi, R. Malhotra, and D. M. Golden, Reaction of chlorine nitrate with hydrogen chloride and water at Antarctic stratospheric temperatures, *Science*, *238*, 1258-1260, 1987.

Toohey, D. W., L. M. Avallone, L. R. Lait, P. A. Newman, M. R. Schoeberl, D. W. Fahey, E. L. Woodbridge, and J.G. Anderson, The seasonal evolution of reactive chlorine in the northern hemisphere stratosphere, *Science*, *261*, 1134-1136, 1993.

Toon, G. C., The JPL MkIV interferometer, *Opt. and Photon. News*, *2*, 19-21, 1991.

Toon, G. C., C. B. Farmer, L. L. Lowes, P. W. Schaper, J.- F. Blavier,

and R H Norton, Infrared aircraft measurements of stratospheric composition over Antarctica during September 1987, *J. Geophys. Res.*, *94*, 7939-7962, 1989.

Toon, G C, J-F Blavier, and J T Szeto, Latitude variations of stratospheric trace gases, *Geophys. Res. Lett.*, *23*, 2599-2602, 1994

Toon, O. B., P. Hamill, R. P Turco, and J. Pinto, Condensation of HNO_3 and HCl in the winter polar stratospheres, *Geophys. Res. Lett.*, *13*, 1284-1287, 1986

Tuck, A. F., R T. Watson, E. P. Condon, J. J Margitan, and O. B. Toon, The planning and execution of ER-2 and DC-8 aircraft flights over Antarctica, August and September 1987, *J. Geophys. Res.*, *94*, 11,181-11,222, 1989

Tuck, A F, C. R. Webster, R. D. May, D. C. Scott, S J Hovde, J. W Elkins, and K. R Chan, Time and temperature dependences of fractional HCl abundances from airborne data in the Southern Hemisphere during 1994, *Faraday Discuss.*, *100*, 389-410, 1995

Tuck, A F, W H. Brune, and R S. Hipskind, Airborn Southern Hemisphere Ozone Experiment/ Measurements for Assessing the Effects of Stratospheric Aircraft (ASHOE/MAESA) A road map, *J Geophys. Res.*, *102*, 3901-3904, 1997

von Clarmann, T, H. Fischer, F Friedlvallon, A Linden, H. Oelhaf, C Piesch, and M. Seefeldner, Retrieval of stratospheric O_3, HNO_3, and $ClONO_3$ profiles from 1992 MIPAS-B limb emission spectra Method, results, and error analysis, *J. Geophys. Res.*, *98*, 20,495-20,506, 1993

Waters, J W., L. Froidevaux, G. L. Manney, W G. Read, and L. S Elson, Stratospheric ClO and O_3 from the Microwave Limb Sounder on the Upper Atmospheric Research Satellite, *Nature*, *362*, 597-602, 1993

Webster, C R., R. D. May, D W Toohey, L M Avallone, J. G Anderson, P Newman, L. Lait, M. R. Schoeberl, J W Elkins, and K R Chan, Chlorine chemistry on polar stratospheric cloud particles in the Arctic vortex, *Science*, *261*, 1130-1134, 1993

Webster, C R, R. D May, C. A. Trimble, R G Chave, and J. Kendall, Aircraft (ER-2) Laser Infrared Absorption Spectrometer (ALIAS) for in situ stratospheric measurements of HCl, N_2O, CH_4, NO_2, and HNO_3, *Appl Opt.*, *33*, 454-472, 1994

Wennberg, P O., R C Cohen, N. L Hazen, L B Lapson, N T Allen, T F Hanisco, J F Oliver, N W. Lanham, J N Demusz, and J G Anderson, Aircraft-borne laser-induced fluorescence instrument for the in situ detection of hydroxyl and hydroperoxyl radicals, *Rev Sci Instrum.*, *65*, 1858-1876, 1994

Woodbridge, E. L., et al., Estimates of total organic and inorganic chlorine in the lower stratosphere from *in situ* measurements during AASE II, *J Geophys Res.*, *100*, 3057-3064, 1995.

World Meteorological Organization (WMO), *WMO Rep. 37, Scientific Assessment of Ozone Depletion: 1994*, Global Ozone Research and Monit Proj., Geneva, 1995

Wornsop, D R, L. E Fox, M S Zahniser, and S. C Wofsy, Vapor pressures of solid hydrates of nitric acid: Implications for polar stratospheric clouds, *Science*, *259*, 71-74, 1993

Zhang, R., P. J. Wooldridge, J P D Abbatt, and M. J Molina, Physical chemistry of the H_2SO_4/H_2O binary system at low temperatures: Stratospheric implications, *J Phys. Chem*, *97*, 7351-7358, 1993.

Zhang, R, M.-T Leu, and M J Molina, Formation of stratospheric clouds on preactivated background aerosols, *Geophys. Res Lett.*, *23*, 1669-1672, 1996.

D Baumgardner and J. E. Dye, National Center for Atmospheric Research, Boulder, CO 80307

K R. Chan and R F Pueschel, NASA Ames Research Center, Moffett Field, CA 94035

R C Cohen, T. F Hanisco, D W Kohn, R M. Stimpfle, and P O. Wennberg, Department of Chemistry, Harvard University, Cambridge, MA 02138

J Elkins, Climate Monitoring and Diagnostic Laboratory, NOAA, Boulder, CO 80303.

S J Hovde, K K Kelly, M. H. Proffitt, and A F Tuck, Aeronomy Laboratory, NOAA, Boulder, CO 80303.

L Jaeglé (corresponding author), Department of Earth and Planetary Sciences, Harvard University, 29 Oxford Street, Pierce Hall, Cambridge, MA 02138 (e-mail:lyj@io harvard.edu)

R D May, R. J Salawitch, D C. Scott, and C. R. Webster, Atmospheric Chemistry Division, Jet Propulsion Laboratory, California Institute of Technology, Pasadena, CA 91109.

J C. Wilson, Department of Engineering, University of Denver, Denver, CO 80208.

Y L. Yung, Division of Geological and Planetary Sciences, California Institute of Technology, Pasadena, CA 91125.

(Received March 20, 1996; revised March 12, 1997;
accepted March 27, 1997)